W-AM-Po54 DETECTION OF A CONFORMATIONAL CHANGE UPON REDUCTION OF CYTOCHROME c UTILIZING SPECTROFLUOROELECTROCHEMICAL TECHNIQUES, Michael J. Simone, Ralph A. Magnotti, William R. Heineman and George P. Kreishman, Department of Chemistry, University of Cincinnati, Cincinnati, Ohio 45221

A conformational change upon reduction of cytochrome c (cyt c) has long been postulated to occur, but direct physical chemical evidence of its existence in solution has been lacking to date. Since fluorescence spectroscopy is extremely sensitive to small conformational changes, an optically transparent thin layer electrode has been developed which is compatible with the optical arrangement of a spectrofluorometer. The fluorescence spectrum of tryptophan-59 of horse heart cyt c is markedly different for the reduced and oxidized states. The fluorescence is attenuated by several factors, namely (1) energy transfer of the fluorescence to the heme and (2) because of the high concentrations used in these studies, quenching by other cyt c's in solution. Taking these two factors into account, the observed fluorescence intensities at a given wavelength can be explained if one assumes a movement of the tryptophan toward the heme of 0.7 $\pm$ 0.3 Å upon reduction.

W-AM-Po55 REDUCTION OF HEME PROTEINS BY CARBON MONOXIDE **D. Bickar, C. Bonaventura, and J. Bonaventura, Duke Univ. Marine Laboratory, Beaufort, N.C. 28516.**

When cytochrome c oxidase is stored in the ferric, Fe(III), form under an atmosphere of carbon monoxide, the heme iron is slowly reduced to Fe(II). Although this phenomena has been often reported, it has never been explained. We propose that this process, termed autoreduction, is due to the heme-catalyzed oxidation of CO to CO2, with the concominant reduction of the ferric heme: 2Fe(III) + CO + H2O -> CO2 + 2H+ + 2Fe(II). We find that ferric iron in other CO-binding heme proteins (hemoglobin and myoglobin) is reduced much more slowly than is cytochrome A3 in the four metal complex of cytochrome c oxidase. Cytochrome c and cytochrome A, which do not bind CO, do not catalyze this reaction. Production of the reaction products, (CO2, protons and ferrous iron) can be inhibited by ligands which bind Fe(III). Under different conditions the reverse reaction, starting with CO2 and Fe(II) and forming Fe(III) and CO, can be observed. These results support our hypothesis for the mechanism for autoreduction. The proposed mechanism implies that autoreduction supplies two electrons per CO oxidation, and redox considerations explain how non-CO binding metal of the cytochrome oxidase complex are reduced. Another implication is an alternative mechanism for cytochrome c oxidase-catalysis of the reaction: 2CO + O2 -> 2CO2. Young and Caughey (Young, L. and Caughey, W. (1980) Fed. Proc. 39, 2090 (Abstr. 2562) have suggested that the reaction is a concerted process, occurring with oxygen and two molecules of CO in the heme A3 site of cytochrome c oxidase. It seems possible, in light of the mechanism of autoreduction, that the process is instead a two step reaction, with an initial reduction of cytochrome c oxidase by CO releasing CO2, followed by oxidation of cytochrome c oxidase by O2. **Research supported by NSF PCM79-06462, NIH HL15460-09**

W-AM-Po56 RESONANCE RAMAN SPECTRA OF HEME c AND HEME d_1 IN PSEUDOMONAS CYTOCHROME OXIDASE Y. Ching, M. R. Ondrias, D. L. Rousseau, Bell Laboratories, Murray Hill, NJ 07974, B. B. Muhoberac, Department of Biochemistry, University of Texas Health Science Center, San Antonio, TX 78284, and D. C. Wharton, Department of Biology, Northeastern University, Boston, MA 02101.

We reported the results of resonance Raman spectroscopic studies of the isolated Pseudomonas cytochrome oxidase. The spectra of the heme c and heme d_1 region of the fully reduced enzyme can be completely separated by using different laser frequencies in the Soret region. The heme c spectrum is very similar to that of cytochrome c and the reduced heme d_1 spectrum is consistent with that of a 5-coordinate high spin species. The number of resonance Raman active vibrations of the heme d_1 moiety far exceeds those apparent in Soret excited scattering from other hemes. The occurrence of a mode in the 1700cm^{-1} region of the heme d_1 suggests the presence of a keto group on the chlorin macrocycle.

There are pronounced spectral changes detected in the heme d_1 region upon binding cyanide to the fully reduced enzyme but there is very little effect on the heme c spectrum. This indicates the lack of significant electronic interaction between heme c and heme d_1. We also obtained the resonance Raman spectra of the heme c and the heme d_1 for the fully oxidized (resting) and NO_2^- bound enzyme. There are distinct differences in the heme d_1 Raman spectra between the nitrite bound and nitrite free enzymes.

W-AM-Po57 NUCLEOTIDE PROBES OF GASTRIC ATPase: G. Sartor, E. Mukidjam, L. Faller, G. Saccomani, G. Sachs. Laboratory of Membrane Biology, UAB, Birmingham, Alabama 35294.

Gastric ($H^+ + K^+$) ATPase has two affinities for ATP in the nanomolar and micromolar range either in the presence or absence of K^+ by steady state kinetic analysis. TNP-ATP is a fluorescent probe of nucleotide sites for various transport ATPases and appears suitable also for the gastric enzyme. Titration of the enzyme in the absence of Mg^{++} showed one class of sites. In the presence of Mg^{++} high and low affinity nucleotide binding was detected. The presence of K^+ reduced the affinity as expected from previous kinetic data. Displacement of bound TNP-ATP in the absence of Mg^{++} revealed one class of low affinity sites for ATP-PCP, ADP or vanadate (a potent inhibitor of the enzyme). In the presence of divalent cation an additional high affinity displacement was seen. TNP-ATP was a competitive inhibitor of the enzyme with K_I values of 10nM and about 1uM. Thus, data with TNP-ATP show the presence of an affinity change for nucleotide, dependent on the presence of Mg^{++}. N_3-ATP also bound to the enzyme in the presence of Mg^{++}. Before photolysis, this nucleotide was a substrate for the enzyme and showed phosphorylation and K^+ dependent dephosphorylation was found. However, of the 5 major peptides detected on isoelectric focussing gels, 2 at pI of 6.0 and 6.8 contained bound nucleotide and corresponded to about 70% of the 100,000 MWt protein in the pI range between 6 and 7. (NIH, NSF, NATO support).

W-AM-Po58 INTERACTION OF N-DANSYL-APOLIPOPROTEIN C-II FRAGMENTS WITH LIPOPROTEIN LIPASE IN THE PRESENCE OF LIPID VESICLES. John C. Voyta. Baylor College of Medicine and The Methodist Hospital, Houston, TX 77030.

Apolipoprotein C-II(apoC-II), a peptide in plasma lipoproteins, enhances lipoprotein lipase hydrolysis of triacylglycerol-rich lipoproteins. For activation of lipoprotein lipase, only the carboxyl third of apoC-II is needed. Carboxyl terminal apoC-II peptides, which do not contain tryptophan, were synthesized by solid phase techniques. As the last step in synthesis, the amino terminal residues were deprotected and acylated with the fluorescent dimethylnapthalenesulfonyl (DNS) group. After chromatography on DEAE-Sepharose in 6 M urea, peptide homogeneity was shown by isoelectric focusing and C_{18} reversed phase HPLC. Activation by apoC-II-DNS(64-78), apoC-II-DNS(60-78), apoC-II-DNS(55-78), apoC-II-DNS(50-78) and apoC-II-DNS(43-78) was 0, 60, 80, 90 and 100% of that produced by native apoC-II. Peptide:lipoprotein lipase interaction was monitored by resonance energy transfer from the tryptophan residues of lipoprotein lipase to the DNS group of apoC-II fragments bound to single-walled vesicles of nonhydrolyzable 1-oleyl-2-phosphorycholine glyceryl ether, trioleylglyceryl ether and cholesterol (molar ratios 1:0.02:0.05). K_a values were <0.01,1,1,1 and 5×10^6 M^{-1}, respectively. The K_a of apoC-II association with apoC-II-DNS(50-78) was 0.1×10^6 M^{-1}. The same chain length dependence of both the energy transfer between lipoprotein lipase and apoC-II at the lipid-water interface and the activation of triglyceride hydrolysis by lipoprotein lipase suggests that enhancement of catalysis involves protein:protein interaction (supported by Welch, USPHS).

W-AM-Po59 PURIFICATION AND CHARACTERIZATION OF AN EXTRACELLULAR PROTEIN KINASE, T. A. SHUSTER, A. NAGY, AND M.D. ROSENBERG, DEPT. GEN. AND CELL BIOL., UNIV. OF MINN., ST. PAUL, MINN. 55108.

A protein kinase (PK) present extracellularly in secretions from the lumen of chicken oviduct has been characterized, purified, and the catalytic portion utilized as an immunogen in rabbits. The PK activity is primarily a type II cAMP dependent protein kinase, very similar to well-studied mammalian enzymes in ion dependency, pH dependency, behavior on ion exchange columns, regulatory subunit autophosphorylation, Ka for cAMP, Km for ATP and subunit molecular weights. The apparent MW (SDS PAGE) for the regulatory subunit is 54,000 daltons and for the catalytic (C) subunit is 40,000 daltons. The holoenzyme is apparently a dimer rather than the expected tetramer (by gel filtration). There is evidence for the presence of protease which could reduce the tetramer to a dimer. The C subunit has been purified more than 7000 fold to greater than 90% homogeneity on SDS PAGE. 10-20 μg of the C subunit was repeatedly injected with adjuvant into the popliteal lymph node of rabbits in either native or SDS denatured form. Both forms were immunogenic. Solid phase antigen binding techniques were used to detect C specific IgG. Either purified C subunit or partially purified enzyme was bound to vinyl microtiter plates, and the binding of diluted preimmune or immune serum was determined using ^{125}I labelled protein A (IPA) as an indicator. Reproducible ratios of 4:1 (immune serum: preimmune serum well) of IPA bound indicate IgG binding to the C subunit. Ratios as high as 7:1 have been obtained. Immune serum binding is dependent upon the number of immunizations and binding declines with time if no boosters are given. Partially purified enzyme yields much lower ratios (1.26:1) indicating some specificity of the antiserum.

W-AM-Po60 ALLOSTERIC INTERACTIONS IN THE PROCESS OF HORMONE INDUCED NUCLEOTIDE EXCHANGE: I. THE REGULATORY ROLE OF GUANINE NUCLEOTIDES. P. M. Lad, D. Reisinger, P. Smiley. Kaiser Regional Research Laboratory and Kaiser Foundation Hospitals, 4953 Sunset Boulevard, Los Angeles, CA 90027.

Treatment of turkey erythrocyte plasma membranes with isoproterenol (Iso) and GMP causes the release of tightly bound GDP and the restoration of regulation of the β-adrenergic receptor and adenylate cyclase by guanine nucleotides. We examined several aspects of this exchange process and observed the following: (a) Incubation of the membrane over 50-fold range of dilution of the plasma membrane at saturating concentrations of Iso showed no exchange. Inclusion of a second nucleotide [GMP or Gpp(NH)p] results in exchange at the lowest dilution. (b) The type of nucleotide influences the rate of the process: GMP (20 min), GDPβS (7 min), Gpp(NH)p (4 min). (c) In sequential treatments with Iso + GMP followed by Gpp(NH)p the index of exchange [ratio of initial rates in the presence of Gpp(NH)p and Iso + Gpp(NH)p] is 1.0. Incubation of these membranes in the absence of Iso causes a decline to an index of 0.7. Inclusion of Iso accelerates the process and causes a change to 0.4. In contrast to the native membrane, inclusion of a second nucleotide (GDP) is now no longer required to achieve exchange. (d) Treatment of the native membrane with EDTA + Iso, or EDTA alone causes no change in the index of exchange. By contrast, EDTA markedly influences the rate and the index of exchange in the presence of membranes sequentially treated with Iso + GMP and then with Gpp(NH)p. (e) Conditions can be devised so that exchange can proceed without loss of activation of adenylate cyclase by fluoride ion. A regulatory role for guanine nucleotide in the exchange process via a sequence of site-site interactions compatible with these observations is proposed.

W-AM-Po61 CONTROLLED SUBTILISIN DIGESTION OF PSEUDOMONAS CYTOCHROME OXIDASE IN THE ABSENCE AND PRESENCE OF THE INHIBITOR KCN. Barry B. Muhoberac, David C. Wharton, Karen Falksen, and Paul M. Horowitz, Department of Biochemistry, The University of Texas Health Science Center at San Antonio, San Antonio, Texas 78284.

Oxidized Pseudomonas cytochrome oxidase was digested with subtilisin under controlled conditions in the absence and presence of KCN and was found to produce discrete, high molecular weight fragments (A and B). The presence of KCN alters the rate of this fragmentation but does not change the nature of the fragments. When digested in the absence of KCN, the oxidase gives a major product (A) which is enzymatically active and has an apparent MW of 58,000 on SDS-polyacrylamide gel electrophoresis (SDS-PAGE). In the presence of KCN the major product (B) has a MW of 48,000 on SDS-PAGE. Furthermore, HPLC gel exclusion chromatography indicates that product B has an apparent MW of 92,000. This implies that product B is dimeric, as is the parent enzyme which has a MW of 110,000 by HPLC. Product B was isolated by gel filtration, and spectral studies show that it contains only the heme d_1 moiety. Evaluation of the digestion time course indicates that the rate at which several minor products are formed is also dependent on the absence or presence of KCN. These observations suggest that the binding of KCN to the heme c-containing portion of the protein, which is at one end of the intact enzyme, can be removed without disrupting the integrity of the heme d_1-containing portion. (Supported by Welch grant AQ-723 and NIH grants GM-25177 and HL-16686.)

W-AM-Po62 NMR STUDIES OF E. COLI ALDOLASE KINETICS. B. Szwergold, K. Ugurbil and T.R. Brown, Dept. of Biochemistry, Columbia University, NY 10032 (B.S. and K.U.) and Bell Laboratories, Murray Hill, N.J. 07974 (T.R.B.)

Fructose 1,6-bisphosphate (Fru-P_2) aldolase has been isolated and purified from E. coli. Preparations with the highest purity gave a specific activity of $\sim$50 I.U. (μmoles of Fru-P_2 cleaved per min per mg protein) when assayed at 30°C in 80 mM glycylglycine buffer, pH 9.0. Saturation transfer measurements have been performed using ^{13}C NMR at 90.52 MHz and [2,5-^{13}C]Fru-P_2. In the presence of $\sim$1000 I.U. per ml of enzyme, $\sim$50% reduction of the intensities of the α and β Fru-P_2-C2 resonances were observed upon saturation of the C2 carbon resonance of the keto form of dihydroxyacetone phosphate (DHAP); no reduction in the Fru-P_2 resonances were detected, however, upon saturation of the C2 resonance of the diol form of DHAP. This result unequivocally demonstrates that the E. coli aldolase utilizes exclusively the keto form of DHAP.

W-AM-Po63 STRUCTURE OF VITAMIN D-DEPENDENT CALCIUM BINDING PROTEIN FROM BOVINE INTESTINE

Szebenyi, D.M.E., Obendorf, S.K. and Moffat, K.,
Section of Biochem., Mol. and Cell Biol., Cornell University, Ithaca, New York 14853

The structure of a vitamin D-dependent calcium binding protein from bovine intestine (ICaBP) has been determined crystallographically to 2.3 Å resolution. ICaBP, whose exact function is not known but which probably concerns regulation of intestinal calcium absorption, belongs to the calmodulin family of calcium binding proteins. These proteins are predicted to contain helix-loop-helix calcium binding domains ("EF hands") similar to those in parvalbumin. ICaBP contains two such domains similar but not identical to the parvalbumin EF hand. The C-terminal domain differs in the exact orientation and positioning of the helices; the N-terminal domain, however, has a calcium binding loop which is two residues longer and uses more main chain carbonyls as calcium ligands. The ICaBP structure thus supports the prediction of widespread occurrence of EF hands, but also reveals the possibility of substantial variation in the conformation of such structures. Removal of one or both calciums from ICaBP alters the protein structure, and we are now attempting to determine the nature of the alterations by crystallizing and studying the monocalcium and calcium-free forms of the protein.

W-AM-Po64 UNUSUAL PRODUCTS FROM CRYSTALLIZED AND SOLUBLE TRYPTOPHAN-tRNA SYNTHETASE FROM BACILLUS STEAROTHERMOPHILUS

D.E. Coleman and C.W. Carter, Jr., Department of Biochemistry 231H, University of North Carolina, Chapel Hill, NC 27514

Tryptophan tRNA synthetase from Bacillus stearothermophilus is found by double-label experiments to produce several unusual products in the presence of tryptophan and high concentrations of ATP. Under low ionic strength acylation conditions the predominant product is tryptophanyl-ATP as is found for E. Coli tryptophan-tRNA synthetase under similar conditions (Joseph, D. R. and Muench, K. H., (1971) J. Biol. Chem. 246, 7610-7615). Crystals of the B. Stearothermophilus enzyme have been grown in the presence of tryptophan, ATP, and 1.9 M potassium phosphate (Carter, C. W. Jr. and Carter, C. W (1979) J. Biol. Chem. 254, 12219-12223). Both crystallized and soluble enzyme in 1.9 M phosphate form tryptophanyl-ATP and additional compounds containing tryptophan. These findings are discussed with respect to the enzymology of the protein and to preliminary x-ray studies of the crystals. (Supported by a grant from the National Institutes of Health (GM 26203)).

W-AM-Po65 KINETIC STEPS IN ATP HYDROLYSIS BY THE RECA PROTEIN OF E. COLI.

Howard White and Arne Strand, Dept. of Biochemistry, University of Arizona, Tucson, Arizona 85721.

Several kinetic phases have been observed during hydrolysis of ATP by the E. coli recA gene product (PrecA) activated by single-stranded DNA (ssDNA). Upon mixing of ATP with PrecA·ssDNA at 37°C in a stopped-flow fluorometer, a phase characterized by a rapid decrease in intensity of scattered light is observed. In the range of ATP concentrations from 0 to 200 μM, this decrease can be described by a second-order rate constant of 6×10^4 $M^{-1}s^{-1}$. Following this initial fast phase, scattering intensity first increases, then plateaus, and finally slowly decreases. The increase in scattering intensity is apparently independent of ATP concentrations above 100 μM and is described by a rate constant of 0.15 s^{-1}, which is approximately equal to the steady-state rate of ssDNA-dependent ATPase activity of PrecA. The subsequent plateau phase is characterized by a constant high level of light scattering for a time which depends on ATP concentration, and is followed by a slow decline in scattering to levels which would be expected from non-interacting PrecA and ssDNA.

These results suggest a mechanism in which an initial PrecA·ssDNA complex is dissociated upon addition of ATP. Second, a rate-limiting formation of a transient PrecA·ssDNA·nucleotide complex occurs. Then after an intervening plateau phase dissociation of the complex occurs at a rate correlated with the depletion of ATP due to hydrolysis. The non-hydrolyzed ATP analog ATP-γS promotes the formation of a stable PrecA·ssDNA·nucleotide complex comparable to the transient complex formed using ATP. (Supported by PHS grant AM25113-01).

W-AM-Po66 ^{13}C NMR STUDIES OF GLYCOLYTIC CONTROL IN YEAST: ^{13}C LABEL DISTRIBUTION IN FRUCTOSE-1,6-BISPHOSPHATE. J.A. den Hollander and R.G. Shulman. Department of Molecular Biophysics and Biochemistry, Yale University, New Haven, CT.

In a previous study (1) it was found that it is possible to observe intracellular fructose-1,6-bisphosphate (Fru-P_2) by ^{13}C NMR in suspensions of intact yeast cells, which are glycolyzing on ^{13}C enriched glucose. The ^{13}C label introduced at either the C_1 or the C_6 positions of glucose appeared in Fru-P_2 in the C_1 and C_6 positions simultaneously. From this "scrambling " of the ^{13}C label it was possible to obtain detailed kinetic information of the <u>in vivo</u> kinetics of Fru-P_2-aldolase and triosephosphate isomerase.

This approach was used in the present study to investigate the control of glycolysis in yeast. Suspensions of catabolite derepressed yeast cells were incubated with [1-^{13}C] glucose, both aerobically and anaerobically. Perchloric acid extracts were taken during steady state glycolysis and the ^{13}C label distributions in Fru-P_2 in the extracts were determined by ^{13}C NMR. The ratio of the C_6 to C_1 intensity in Fru-P_2 was 0.5 in the anaerobic case, and 0.8 aerobically. From this it is concluded that upon oxygenation there is a reduction of the apparent rate constant of glyceraldehyde-3-phosphate dehydrogenase by about a factor 3. This agrees with the reduction in glucose flow through PFK, which has also been shown to decrease by a factor of ∿3 upon oxygenation, (2) and is consistent with the rather constant levels of Fru-P_2 in these samples.

[1]J.A. den Hollander, T.R. Brown, K. Ugurbil and R.G. Shulman (1979) Proc. Natl. Acad. Sci. USA 76: 6096-6100.

[2]J.A. den Hollander, K. Ugurbil, T.R. Brown and R.G. Shulman (1981) Biochemistry 20: 5871-5880.

W-AM-Po67 A ^{1}H NMR STUDY OF THE LANTHANIDE INDUCED SHIFTS OF YTTERBIUM SUBSTITUTED PARVALBUMIN AND THE ELUCIDATION OF THE PRINCIPAL ELEMENTS AND ORIENTATION OF THE MAGNETIC SUSCEPTIBILITY TENSOR OF THE METAL ION. L. Lee and B.D. Sykes, M.R.C. Group on Protein Structure and Function, The University of Alberta, Biochemistry Department, Edmonton, Alberta, Canada T6G 2H7.

The substitution of the lanthanide ion ytterbium for the calcium ion in the EF binding site of carp parvalbumin results in high resolution ^{1}H NMR spectra exhibiting a series of resonances with chemical shifts spread over the range 32 to -19 ppm. The paramagnetic induced shifts are sensitive monitors of the precise geometrical orientation of each proton nucleus relative to the metal. Interpretation of the shifts in geometric terms require knowledge of the orientation and principal elements of the ytterbium magnetic susceptibility tensor. We have revised our original principal axis system (PAS), which was determined using the three assigned NMR resonances [the His 26 C-2 and C-4 protons, and the amino terminal acetyl protons] and seven methyl groups with known geometry relative to the EF metal binding site, by including new assigned resonances including the ^{113}Cd NMR resonance of Cd(II) bound to the CD site, a ^{13}C NMR resonance from ARG 75, and a ^{19}F NMR resonance from labelled CYS 18. The elucidation of this PAS has allowed us to view the coordination geometry of the metal binding site and to compare the observed spectrum of the nuclei surrounding the EF metal binding site of parvalbumin with that spectrum calculated from the X-ray crystallographic structure. The overall agreement between the x-ray and solution structures is much improved with our new PAS, although specific residues are different in solution.

W-AM-Po68 A PRELIMINARY ANALYSIS OF <u>TARICHA GRANULOSA</u> SKILTON PLASMA PROTEINS USING ONE AND TWO DIMENSIONAL POLYACRYLEMIDE GEL ELECTROPHONESIS - G.B. Friedmann, Physics Department, University of Victoria, Victoria, B.C., Canada, V8W 2Y2 (Intr. by H.S. Sandhu).

Preliminary evidence for the possibility of at least three light weight immunoglobins (molecular weights of 112 - 120,000, 155-160,000 and 165-175,000 daltons of the form L_2 H_2 having components in the 56-61,000, 37-38,000 and 24-26,000 dalton region and of a coagulation protein with sub units of 51,000 and 54,000 daltons in the plasma of <u>Taricha granulosa</u> Skilton blood is presented. Such immunoglobins have not previously been seen in these amphibians, but compare to IgY polypeptides found in larval frogs and some birds. The coagulation proteins seem to react similar to mammalian counterparts. Some implications for evolution theories and clotting mechanisms will be discussed.

W-AM-Po69 OXYGEN QUENCHING OF SENSITIZED TERBIUM LUMINESCENCE IN COMPLEXES OF TERBIUM WITH SMALL ORGANIC LIGANDS AND PROTEINS. F. G. Prendergast, Dept. of Pharmacology, Mayo Foundation, Rochester, MN 55905.

We have used oxygen quenching to investigate energy transfer to terbium in complexes of this ion with low molecular weight organic ligands and with four proteins, elastase, α-amylase, thermolysin, and apo-transferrin. Oxygen does not quench the luminescence of free terbium and only minimally quenches the luminescence of Tb^{3+} complexed to dipicolinic acid. Stern-Volmer plots of oxygen quenching of terbium luminescence in elastase-Tb, α-amylase-Tb, and apo-thermolysin-Tb complexes are clearly biphasic. The majority of the Tb^{3+} luminescence is lost at low oxygen pressures (< 150 psi) but the plots become more flattened with smaller slopes at higher oxygen pressures. The Stern-Volmer plots of oxygen quenching of intrinsic (tryptophan) fluorescence in complexes of Tb^{3+} with elastase and apo-thermolysin are linear. They exhibit slopes that are smaller than those of the initial phase of quenching of the luminescence of terbium, but are grossly similar to the limiting slopes seen in the Stern-Volmer plots for Tb^{3+} luminescence loss. In α-amylase where energy transfer is also apparently from tryptophan residues, Tb^{3+} luminescence is obviously more sensitive to the effects of oxygen than is intrinsic tryptophan fluorescence, but not as markedly as in elastase and thermolysin. We propose that in the elastase and thermolysin energy transfer occurs mainly from excited triplet states of tryptophan. For α-amylase our data support energy transfer mainly from singlet tryptophan. This work was supported in part by NSF Grant PCM 7911492 and the Mayo Foundation. F.G.P. is an Established Investigator of the American Heart Association and a Searle Foundation Scholar.

W-AM-Po70 MEASUREMENT OF ELECTROSTATIC AND VAN DER WAALS FORCES IN TMV GELS. B. M. Millman, T. C. Irving, B. G. Nickel and M. Loosley-Millman. Biophysics Interdepartmental Group, Physics Department, University of Guelph, Guelph, Ontario, Canada, N1G 2W1.

Lattice pressure as a function of interrod spacing has been measured in hexagonal gels of tobacco mosaic virus by an osmotic stress technique. Experimental curves relating the logarithm of lattice pressure to interrod spacing have been compared to similar curves calculated for electrostatic and van der Waals pressures (Millman and Nickel, 1980, Biophys. J. 32:49) assuming a rod radius of 9 nm, rod charge of 2 electrons/subunit and Debye constants calculated from the ionic strength of the solutions. Lattice pressure increases with decreasing interrod spacing, the slope of the curve depending on the ionic strength (I). The slopes of the experimental curves decrease with decreasing I (1.0 - 0.001 M), agreeing well with the calculated slopes, though some discrepancy was observed at the ends of the range. The curves lie at the predicted spacings for I = 0.1 - 0.001 M and pH 6. As the pH is shifted (5 - 8), the slope is unchanged, but the curves shift in position more than predicted from the changes in rod charge calculated from electrophoretic mobilities. Internal lattice attractive pressures were determined from extrapolation of electrostatic pressure curves to the spacings observed at zero external pressure and were compared to calculated van der Waals pressures. Good agreement was obtained at high I, but at low I the observed pressure was greater than the calculated van der Waals pressure. We conclude that in TMV gels near physiological conditions the gel spacing (with no external pressure) is a result of a force balance between electrostatic and van der Waals forces. In other regimes, either the calculated forces need to be modified or some other forces are involved.

W-AM-Po71 SPECTROSCOPIC STUDIES AND CHARACTERIZATION OF THE LIPOPROTEIN COMPLEX FORMED BY GLUCAGON AND DICAPRYL PHOSPHATIDYL CHOLINE. J.R. Ernandes, Inst. de Química, Universidade Estadual Paulista, Araraquara, BRAZIL, S. Schreier, Inst. de Química, Universidade de São Paulo, São Paulo, BRAZIL, and R.M. Epand, Dept. of Biochemistry, McMaster University, Hamilton, CANADA (Intr. by R. Meneghini).

The interaction between glucagon and dicapryl phosphatidyl choline (DCPC) was studied by fluorescence, circular dichroism (CD), ^{1}H and ^{31}P NMR. The lipoprotein complex was characterized by gel filtration and ultracentrifugation. The fluorescence spectra of glucagon in the presence of DCPC suggest that Trp-25 is in a more hydrophobic environment. In addition, the far and near UV CD spectra of glucagon show an increased helix content and the aromatic residues in a more structured environment. The ^{1}H NMR spectra suggest that the C-terminal region and the aromatic residues of glucagon are involved in the interaction with the phospholipid. The ^{31}P resonance of DCPC in the complex is narrower than in sonicated vesicles; in addition, ^{1}H-^{31}P coupling is observed in the former system. These results are in agreement with gel filtration experiments which suggest that DCPC is "solubilized" by glucagon giving rise to a lipoprotein complex which is smaller than the original DCPC aggregates. Density pertubation sedimentation equilibrium indicates that the complex consists of 7±1 glucagon and 19±7 DCPC molecules.

JRE was partly supported by the exchange programme between the NRC of Canada and the CNPq of Brazil.

W-AM-Po72 ANALYSIS OF NMR RELAXATION DATA ON MACROMOLECULES USING THE MODEL-FREE APPROACH.
Giovanni Lipari and Attila Szabo, Laboratory of Chemical Physics, NIADDK, National Institutes of Health, Bethesda, Maryland 20205.

The model-free approach to the interpretation of NMR relaxation data in solution is based on the result that the unique information on fast internal motions contained in relaxation experiments can be completely specified by two model-independent quantities (1) a generalized order parameter, S, which is a measure of the spatial restriction of the motion and (2) an effective correlation time, τ_e, which is a measure of the rate of motion. Here we deal with the extraction and interpretation of this information. The procedure to obtain S^2 and τ_e from experimental data by a least-squares method and, in certain favorable circumstances, by using an analytical formula is described. A variety of experiments are then analyzed to yield information on the time scale and spatial restriction of internal motions of isoleucines in myoglobin, methionines in dihydrofolate reductase and myoglobin, a number of aliphatic residues in basic pancreatic trypsin inhibitor, ethyl isocyanide bound to myoglobin and hemoglobin and aliphatic side chains in three random-coil polymers. The numerical values of S^2 and τ_e can be readily interpreted within the framework of a variety of models. In this way one can obtain the same physical picture of internal motions as that obtained by fitting the data using complicated spectral densities. The numerical value of the order parameter, unlike the effective correlation time τ_e, plays a crucial role in determining what models can be used to describe the experiment: models in which the order parameter cannot be reproduced are eliminated. Conversely, any model that can yield the correct value of S^2 works.

W-AM-Po73 COMPETITION AND GATING IN DIFFUSION CONTROLLED REACTIONS. David Shoup and Attila Szabo, Laboratory of Chemical Physics, NIADDK, National Institutes of Health, Bethesda, Maryland 20205.

The time-dependence and steady state association and dissociation constants are obtained for a variety of diffusion controlled reactions of biophysical interest. Specifically, we consider the reaction of a small ligand with a system containing one or more localized reactive sites including the possibility that the reactivity of these sites can fluctuate in time. The competition between reactive sites on a macromolecular surface is treated by using the so-called radiation boundary condition (i.e. the macromolecule is partially reactive because its surface is partially covered by reactive sites). The resulting rate constant is shown to be the same as that for two consecutive pseudo-first order reactions (i.e. the ligand first diffuses to the macromolecule and then it reacts with a certain rate). A new approach to the calculation of dissociation rates is presented. This approach (which is based on a simple but rigorous expression for the equilibrium constant derived using statistical mechanics) can handle single and multiple sites with equal ease and is free of ambiguities inherent in the conventional treatment. Finally, the rate constant for the reaction of a small ligand and a system with a gate (e.g. the entrance to the pocket in myoglobin or a channel in a membrane) is calculated under the assumption that the opening and closing of the gate is a stationary Markov process. The limits when the relaxation time describing the fluctuations of the gate is either smaller or larger than the characteristic time for diffusion are discussed.

W-AM-Po74 THE ROLE OF IRON IN THE FUNCTION OF PHENYLALANINE HYDROXYLASE: EPR STUDIES
by Betty Jean Gaffney*, D. Wallick**, R. Lazarus** and Stephen J. Benkovic**, Chemistry Departments, The Johns Hopkins University*, Baltimore, Maryland 21218 and Pennsylvania State University**, University Park, Pennsylvania 16802.

Phenylalanine hydroxylase contains four iron atoms per tetramer. Electron paramagnetic resonance (EPR) spectra have been measured at temperatures from 4 to 70 K for the enzyme in the presence or absence of substrates and cofactors. In the presence of oxygen and the absence of phenylalanine or 6-methyltetrahydropterin, the enzyme exhibits a signal dominated by a peak of ~45 gauss width (peak to peak) at g_{eff} = ~4.3. As the enzyme is titrated with phenylalanine, the signal sharpens to a width of ~40 gauss. Further sharpening to ~25 gauss results when the pterin cofactor is added. The temperature dependencies, power saturations and signal intensities during titrations all suggest that the iron atoms on separate subunits act independently and that changes in coordination to iron accompany catalysis by this enzyme.

W-AM-Po75 TRYPTOPHAN AND TYROSINE RESIDUES IN LENS PROTEINS AND ITS SUSCEPTIBILITY TO PHOTOOXIDATION. J.N. Liang and B. Chakrabarti, Eye Research Inst., Boston, MA. 02114

Circular dichroism (CD) and fluorescence measurements have been carried out to study the tertiary structure and environments of aromatic amino acid residues of lens proteins, α, β_H, β_L and γ-crystallins. The near-UV CD spectra which arise mostly from aromatic amino acid residues, differ considerably from each other and the differences reflect the extent of interaction (u-u coupling) between these residues of each protein; there is no significant contribution of the disulfide bond. The CD spectra further indicate that the tryptophan residues in γ-crystallin are mostly buri ed in a hydrophobic environment, wherease in α-crystallin, they are least buried. On the other hand, tyrosine residues in both of the β-crystallins are in polar environments than are in the α- and γ-crystallins.

The emission maxima and quantum yield values of the fluorescence of lens crystallins similarly suggest that the order of exposed tryptophan residues in these proteins are: $\alpha > \beta_H \simeq \beta_L > \gamma$. Because of efficient energy transfer from tyrosine to tryptophan in these proteins, tyrosine fluorescence can be observed only when they are measured in guanidine hydrochloride.

The implied significance of the study is that the tryptophan residues of crystallins suffer photooxidative changes by sunlight leading to cataract formation. We have observed that the rate of tryptophan photooxidation, upon irradiation of lens crystallin by UV light (300 nm), is maximum in α-crystallin compared to other two crystallins, as expected from the results of CD and fluorescence.

W-AM-Po76 X-RAY SCATTERING FROM BIOMOLECULES IN SOLUTION: APPLICATION TO THE STUDY OF MOLECULAR CONFORMATION AND DYNAMICS. C.A. Pickover and D.M. Engelman, Department of Molecular Biophysics and Biochemistry, Yale University, New Haven, Connecticut 06511

Among the methods available for the structural characterization of proteins, lipoproteins, nucleic acids, and viruses, x-ray solution scattering is emerging as an important tool. If solution scattering curves can be accurately predicted from structural models, measurements can provide useful tests of predictions of secondary and tertiary structure. A computational technique for the prediction and interpretation of x-ray scattering profiles from biomolecules in solution has been developed. The method employs a Monte Carlo procedure for the generation of length distribution functions and provides predictions to moderate resolution (5 angstroms). Predicted scattering profiles of lysozyme and bovine pancreatic trypsin inhibitor (BPTI) compare extremely well with experimental scattering curves obtained from these proteins in solution measured using photographic film techniques. In comparing observed and calculated scattering curves for a protein in solution, the effect of protein motion must be considered. This problem has been approached by calculating scattering curves for several consecutive 0.147 picosecond atomic coordinate frames from a molecular dynamics simulation of the motion of BPTI.

W-AM-Po77 PREPARATION AND CHARACTERIZATION OF GLUCAGON DERIVATIVES FOR SEMISYNTHESIS AND FLUORESCENT LABELLING STUDIES. Kathleen Corey Flanders, Doreen Hung Mar, Rodney J. Folz, Richard D. England, Sharon A. Coolican, Alton D. Floyd and Ruth S. Gurd. (Medical Sciences Program and Department of Chemistry, Indiana University, Bloomington, IN 47405.)

Highly purified N^{ϵ}-acetimidoglucagon has been prepared to assess the role of lysine^{12} in biological activity and for use in semisynthesis. Glucagon reacted with a 50-fold excess of methyl acetimidate (pH 10.2) resulted in preferential acetimidation of the sole ε-amino group. N^{ϵ}-Acetimidoglucagon, isolated by anion-exchange chromatography (pH 9.4), was homogeneous upon isoelectric focusing. The peptide was obtained in 75% yield with greater than 97% of the lysine acetimidated as judged by amino acid analysis following enzymatic digestion. N^{ϵ}-Acetimidoglucagon was equipotent with native glucagon in binding to rat liver plasma membranes and activating adenylate cyclase, eliminating a need for subsequent deprotection.

The acetimidated derivative was reacted with a 25-fold excess of N-hydroxysuccinimidobiotin to produce N^{α}-biotinyl, N^{ϵ}-acetimidoglucagon which was purified by cation-exchange chromatography in 90% yield. The purified product had a pI of 4.6, exhibited 0.2% of the binding affinity and biological potency of native glucagon and was a partial agonist with 30% of the maximum activity of the native hormone. Histochemical localization of N^{α}-biotinyl, N^{ϵ}-acetimidoglucagon in biological tissues with either light or electron microscopic techniques may be demonstrated using avidin labelled with fluorescent compounds or colloidal gold, respectively. (Supported by USPHS, NIH Grant AM 21121. R.D.E. was supported by American United Life through the Insurance Medical Scientist Scholarship Fund.)

W-AM-Po78 INFRARED STUDIES OF BACTERIORHODOPSIN. Gavin Dollinger, Kimberly Bagley, Samuel F. Bowne, Laura Eisenstein, Werner Mäntele, Erramilli Shyamsunder and Fritz Siebert, Department of Physics, University of Illinois at Urbana-Champaign, Urbana Illinois 61801 and Institut für Biophysik und Strahlenbiologie der Universität Freiburg im Breisgau, Albertstrasse 23, D-7800 Freiburg, Federal Republic of Germany.

Infrared difference spectra between light adapted bacteriorhodopsin and various intermediates of its photocycle were obtained at low temperature (70 K - 250 K). The region between 4000 cm^{-1} and 1000 cm^{-1} was studied with a resolution of 2 cm^{-1} using a Nicolet 7760 Fourier-transform IR spectrophotometer. The sample was a hydrated or deuterated film of native or chemically modified bacteriorhodopsin on a CaF_2 window. After light adapting or dark adapting at 300 K, the sample was cooled to a temperature where the intermediate to be studied is thermally stable. After collecting a spectrum of the initial state, a photosteady state containing the intermediate of interest was created using light of the appropriate wavelength. The photosteady state was then scanned and the difference spectrum computed. As a control, the experiments were repeated in the visible region using a Cary 14 spectrophotometer. The data agree with Resonance Raman results in the fingerprint region (1400 - 1000 cm^{-1}) and the ethylenic stretching frequency of the intermediates correlates well with the absorption maximum in the visible. Interpretation of the spectra in the Schiff base region in terms of the protonation state of the various intermediates will be presented. (Supported in part by the U.S. Department of Health and Human Services under Grant No. 5 R01 GM 18051 and by the National Science Foundation under Grants No. PCM 79-05072 and INT 78-27606.

W-AM-Po79 Creatine Kinase In Maturing Mouse Oocyte Bornslaeger, E; Schultz, R.M.; and Iyengar,M.R. (Intr. by Dr. S. Davidheiser) Dept. Biology and Dept. Animal Biology, Univ. of Pennsylvania, Phila., Pa. 19104

A high level of CK activity has been found in the mature mouse ovum and in the early preimplantation embryo (Iyengar, M.R. et al in press). In an attempt to establish the pattern of enzyme change during oocyte maturation, a study was undertaken to determine the cell volume and enzyme activity simultaneously. Oocytes were collected from Swiss-Webster random bred albino mice (8 to 22 days old). Radii of the cells were determined optically and the volumes of the equivalent spheres were computed. CK activity was determined spectrophotometrically by coupling rate of ATP synthesis to NADP reduction. We have observed (i) about a five fold increase in volume between 8 and 22 days (from 40-50 pl to 190-200 pl); and (ii) approximately 3 fold increase in the CK activity from (10 pmole/min/oocyte to 32 pmole/min/oocyte). However the accumulation of the enzyme was non-linear in relation to the increase in volume. The specific activity (2 to 3 umole/min/mg protein) of the mature ovum in these studies were similar to those previously found by Iyengar et al.

W-AM-Po80 THE IN VITRO FORMATION OF VINBLASTINE-INDUCED TUBULIN PARACRYSTALS, George C. Na and Serge N. Timasheff, Graduate Department of Biochemistry, Brandeis University, Waltham, MA 02254

Calf brain tubulin, purified by the modified Weisenberg method, has been successfully induced in vitro to form paracrystalline aggregates with the anti-cancer drug vinblastine. The birefringent paracrystals formed in vitro have a short-rod structure with a hexagonal cross-section and consist of longitudinally packed fibrils. The vinblastine stoichiometry in the paracrystals is a function of the total vinblastine concentration used in growing them. Below 2 x 10^{-4}M vinblastine, the paracrystals contain a rather constant 1.1 $\pm$ 0.2 mole vinblastine per mole of tubulin dimers. From 2 x 10^{-4}M to 10^{-3}M vinblastine, the stoichiometry gradually increases to 1.8 $\pm$ 0.2 mole vinblastine per mole of tubulin. The in vitro formation of the vinblastine-tubulin paracrystals can proceed at 4°C, and it requires the presence of divalent cations, either magnesium or calcium. Similar paracrystals can be formed with vincristine and desacetylvinblastine but not with colchicine or podophyllotoxin. (This work was supported by grants from the National Institutes of Health, CA 16707 and GM 14603).

W-AM-Po81 TERBIUM BINDING TO PERIPHERAL ANIONIC SITES OF RAT BRAIN ACETYLCHOLINESTERASE (AChE). Judith K. Marquis and Andrew J. Lerrick, Dept. of Pharmacology and Experimental Therapeutics, Boston University School of Medicine, Boston, MA 02118.

Terbium has been used as a fluorescence probe of Ca^{2+}-binding sites in many enzyme proteins and membrane-complexed macromolecules. Studies are in progress to characterize the nature of ligand interactions at peripheral anionic sites on mammalian brain AChE, including the β-anionic or "accelerator" anionic sites where enzyme activity is increased upon Ca^{2+} binding. Scatchard analysis of Tb^{3+}-binding to AChE purified from rat brain by affinity chromatography on Concanavalin A-Sepharose 4B (spec. act: 228μmols/hr/mg protein) revealed at least two populations of binding sites: "high affinity" sites with a $K_{d_{app}} \simeq 3.9\mu M$ and "low affinity" sites with a $K_{d_{app}} \simeq 20.7\mu M$. High affinity binding was completely inhibited by Ca^{2+} ($K_{i_{app}} \simeq 2.6$ mM) and displaced by EDTA. Decamethonium appears to inhibit only the nonspecific low affinity component of Tb^{3+} binding. The high affinity binding sites were found to be stable to long-term freezing at -5°C. Control binding of Tb^{3+} was assayed in low ionic strength 2 mM Pipes buffer, pH 6.8. When binding was measured under varied ionic conditions, including 2 mM $CaCl_2$, 16.5 mM NaCl and 67 mM NaCl, a single Tb^{3+} binding component was evident with $K_{d_{app}}$'s between 39μM and 47 μM. Tb^{3+} binding was also measured to a more highly purified enzyme fraction (spec. act: 3,229 μmols/hr/mg protein) obtained by affinity chromatography on m-dimethylaminoethyl benzoate-Sepharose 4B. Scatchard analysis again revealed at least two populations of binding sites with $K_{d_{app}}$'s of 7.6 μM and 49.6 μM. Tb^{3+} binding to this enzyme preparation was also completely displaced by 1 mM EDTA. (Supported in part by DOD-ARO contract #DAAG-29-81-K-0130.)

W-AM-Po82 PROPRANOLOL AND PROGESTERONE BINDING TO OROSOMUCOID. E. D. Sprague, T. L. Kirley and H. B. Halsall, Department of Chemistry, University of Cincinnati, Cincinnati, OH 45221.

As part of a systematic study of the interaction domains of human orosomucoid (OMD) we have investigated its binding to spin-labelled propranolol and spin-labelled progesterone as a function of temperature by electron spin resonance techniques. At 20°C the association constants are $1.9 \times 10^6\ M^{-1}$ and $4.9 \times 10^5\ M^{-1}$, respectively, In each case, the binding is competitive with unlabelled ligand. Above about 50°C the apparent association constant for both ligands decreases rapidly with increasing temperature, thereby yielding a highly non-linear van't Hoff plot over the range 4-70°C. This is due to thermal denaturation of the OMD, as was shown independently by ultraviolet absorption spectroscopy and differential scanning calorimetry. Statistical fitting of the binding data to a model which incorporated a two-state denaturation transition showed excellent correspondence in binding parameters and the independently determined denaturation parameters. Scatchard analysis revealed that below the denaturation region the number of binding sites per OMD molecule remains constant at one. At 37°C, examination of the thermodynamic parameters for binding shows that the binding of progesterone is primarily enthalpically driven, while the binding of propranolol has a substantial entropic component.

Supported by NIH Grant HD 13207

W-AM-Po83 SELF-ASSEMBLY OF SUBUNIT IV OF *LIMULUS POLYPHEMUS* HEMOCYANIN. **Michael Brenowitz, Celia Bonaventura, Joseph Bonaventura Duke University Marine Laboratory, Beaufort, NC 28516**

Hemocyanins are heteropolymers whose oxygen binding and assembly processes reflect the heterogeneity of the constituent subunits. Subunit IV is one of the 8 immunologically distinct subunits of the 48 subunit oligomer of *Limulus* hemocyanin. These studies on purified *Limulus* subunit IV allow the analysis of assembly and allosteric control of function in the absence of subunit diversity. The 5.4S monomer of subunit IV, present at pH 5 and 9, forms hexamers at intermediate pH values. The assembly is a slowly equilibrating equilibrium which shows the mass action dependence expected for a monomer-hexamer interaction. Isolated monomers reequilibrate to the expected monomer-hexamer ratio at a given pH. A good fit to the data was obtained with the uptake of 1 proton per 2 monomers on assembly from alkaline pH and the loss of 1 proton per monomer on assembly from acid pH.

Without calcium the hexamers are noncooperative and have slightly higher oxygen affinity than the monomers. When calcium is present, the hexamers show cooperative oxygen binding with $n_{50} = 1.38$ at pH 7.45. We note that the assembly and function of *Limulus* IV closely resembles that of the native hexamers of *Bathynomus gigateus* hemocyanin indicating that heterogeneity need not be present for cooperative oxygen binding.

This work was supported by NSF grant PCM 7906463.

W-AM-Po84 VIRAL SRC GENE PRODUCTS ARE RELATED TO THE CATALYTIC CHAIN OF BOVINE CYCLIC AMP-DEPENDENT PROTEIN KINASE. Winona C. Barker and Margaret O. Dayhoff. National Biomedical Research Foundation, 3900 Reservoir Road NW, Washington DC 20007

In the process of screening newly determined protein sequences, we noted regions of similarity between the catalytic chain of bovine cyclic AMP-dependent protein kinase (BOV-PK) and the src gene products (transforming proteins) of Moloney murine sarcoma virus and Rous avian sarcoma virus. The avian viral protein is a protein kinase, catalyzing the phosphorylation of tyrosine, whereas BOV-PK phosphorylates serine residues. Using our computer program RELATE, we found that the probability of the avian virus transforming protein being so similar to the others by chance is $<10^{-9}$. These proteins appear unrelated to other sequenced viral proteins tested, some of which also have transforming activity. Furthermore, BOV-PK is unrelated to other kinase sequences in the database. When residues 33-258 of BOV-PK are aligned with 85-329 of the murine virus transforming protein and 259-485 of the avian virus protein, there are 21-24% identities between any two of the sequences. The lysine residue that binds ATP in BOV-PK is conserved in the viral sequences. It is generally believed that the src genes originated from genes in the host DNA. These host genes may be members of a superfamily of distantly related protein kinases that are normal constituents of mammalian cells. Certain of these, particularly those specific for tyrosine, may become oncogenic when the normal control of their expression is deranged by incorporation into a viral genome. (Supported by NIH grants HD09547 and GM08710.)

W-AM-Po85 pH DEPENDENT BEHAVIOR OF PURIFIED BIOSYNTHETIC HUMAN LEUKOCYTE INTERFERON A (LIF-A). S.J. Shire, Protein Chem., Genentech Inc., 460 Pt. San Bruno Blvd., S. San Francisco,CA. 94080

A great deal of research has been performed on various human interferons obtained from human cell cultures (1). Lack of purity as well as quantity of material has impeded attempts to characterize the molecule using the various physical techniques employed by biophysical chemists. With the advent of recombinant DNA technology it has been possible to obtain enough LIF-A at sufficiently high purity to characterize the molecule via physical methods (2). We wish to report here on preliminary potentiometric hydrogen ion titration and analytical sedimentation velocity studies of recombinant LIF-A purified from E. coli extracts. The titration studies which were performed in 0.1N KCl at 25° C yield titration curves which are completely reversible in the acid region. Analysis of the curve in the pH range of 5.5 to 3.5 yields a value for the electrostatic interaction parameter of 0.06, in good agreement with the computed value of 0.07. Below a pH of 3.5 there is a large reduction in this parameter which may reflect an overall swelling of the molecule. An analysis of the neutral region of the derivative curve ($-dpH/d\bar{Z}$ vs $\bar{Z}$) suggests that there exists two or three abnormally titrating amino acids. In order to obtain additional structural information as a function of pH, sedimentation velocity experiments were performed in buffered 0.1N KCl (buffer salts at 0.01M) and reveal pH dependent aggregation. In particular, LIF-A at a concentration of 0.2 to 0.4 mg/ml sediments at a pH of 2.4 with an $S_{20,w}$ value of 1.9 S whereas at a pH of 6.9 the $S_{20,w}$ value = 3.8 S, which suggests formation of dimer or trimer at physiological pH values. This behavior might have ramifications with regard to the mode of interferon action as well as stability and storage.

(1) E. Knight Jr. in Interferon 2 1980 pages 1-11 ed. Ion Gresser, Academic Press.
(2) R. Wetzel et. al. J. Interferon Res. 1, 381 (1981).

W-AM-Po86 ^{15}N and ^{14}N DOUBLE SPIN LABEL STUDIES OF SERUM ALBUMIN - POTENTIAL NEW APPLICATIONS OF DOXYLSTEARATES IN PLASMA PROTEIN AND MEMBRANE STUDIES
J. Carleton Hsia, S.S. Er and D.O. Tinker, Biosciences Division, Defence and Civil Institute of Environmental Medicine, Downsview, Ontario and Department of Biochemistry, University of Toronto, Toronto, Ontario

With the use of a dianionic spin label (1-L-glutamate-5-N-(1-oxyl-2,2,6,6-tetramethy-4-aminopiperidinyl)-2,4-dinitrobenzene (L-Glu-DNB-SL) we have discovered that cis-Parinarate (cis,trans,-trans,cis-9,11,13,15-octadecatetraenoic acid) does not behave like stearate in terms of its binding specificity to human serum albumin (J. Biol. Chem. 256: 2242 (1981). A ^{15}N analogue of L-Glu-DNB-(^{15}N)-SL was synthesized to determine if the position (i) of the doxyl group (N) from the carboxyl group on the stearate (S) (5NS, 7NS, 10NS, 12NS and 16NS) affect their binding specificity to albumin as compared to that of stearate. Stearate is known to enhance L-Glu-DNB-SL binding to albumin. The order of doxylstearate to enhance L-Glu-DNB-(^{15}N)-SL binding to albumin are (10NS ≃ 12NS) > (5NS ≃ 7NS). In fact 16NS like cis-Parinarate inhibits the L-Glu-DNB-(^{15}N)-SL binding to albumin. We show 10NS and 12NS behave more like saturated long chain fatty acids and 16NS behaves like polyunsaturated fatty acids in their binding specificity to serum albumin. In conclusion, a double (^{15}N and ^{14}N) spin label experiment has been successfully performed due to unique separation of the resonance peaks. It would be of interest to see if more refined information can be obtained in lipid-protein interaction based on the present findings (supported in part by MA-4129 from MRC Canada).

W-AM-Po87 REGIONS IN THE CALMODULIN MOLECULE THAT INTERACT WITH ITS TARGET PROTEINS. **W. Drabikowski, Z. Dobrowolski and H. Brzeska. Department of Biochemistry of Nervous System and Muscle, Nencki Institute of Experimental Biology, Warsaw, Poland (Intr. by K. Miki).**

Cleavage of bovine brain calmodulin with trypsin yields proteolytic fragments containing amino acid residues 1-77 (Ca^{2+}-binding regions I,II), 1-90 (regions I,II plus the N-terminal half of region III), 1-106 (regions I,II and III), 78-148 (regions III and IV) and 107-148 (region IV and C-terminal half of region III). We have compared the ability of these fragments to substitue for intact calmodulin in binding troponin I, myelin basic protein and histone H2B, by means of polyacrylamide gel electrophoresis. No binding was detected for fragment 1-77, except in case of histone H2B which formed complexes with all fragments studied. Differences in stability of the complexes of other fragments indicate that region III forms the strongest Ca^{2+}-dependent interprotein interactions. In activating myosin light chain kinase, phosphorylase kinase, and cyclic nucleotide phosphodiesterase, the most effective fragments, in terms of the amount neded for half maximal acivation of the enzyme, were also those containing region III, although even the most effective ones viz. 78-148 and 1-106 required 100-200 times higher concentration than intact calmodulin. These data suggest that region III is essential and other regions of calmodulin may be required for binding or activation of a given target protein.

W-AM-Po88 INTERACTION BETWEEN FIBRONECTIN AND GELATIN IN SOLUTION. Hilda Forastieri and Kenneth C. Ingham, American Red Cross Blood Services, Bethesda, MD 20814.

Fibronectin (Fn) is a large (440 kd) multidomain glycoprotein which interacts with collagen and other constituents of the extracellular matrix and facilitates the adhesion of cells to various surfaces. Most studies of the binding properties of Fn have utilized methods whereby one or the other macromolecule was immobilized on a solid phase. In order to examine the interaction between Fn and gelatin in solution, commercial grade swine skin gelatin (Sigma, type I) was labeled with fluorescein isothiocyanate and fractionated by exclusion chromatography. High and low molecular weight fractions ($\sim 10^{-9}$ M ea) were titrated with affinity-purified human plasma Fn using fluorescence polarization (P) to monitor the interaction in 0.1M Tris buffer, 0.15M NaCl, pH 7.3. The two fractions exhibited similar sigmoidal increases in P (apparent positive cooperativity) with 50% saturation near 10^{-9} and 10^{-8} M Fn respectively. By contrast, a 42 kd chymotrypsin-generated fragment which retains the ability to adhere to gelatin-Sepharose exhibited normal (noncooperative) binding to both fractions with $K_d = 1 \times 10^{-6}$ M. In all cases, the increase in P could be reversed by addition of excess unlabeled gelatin.

At higher concentration ($>10^{-8}$ M), P for the high molecular weight fraction increased linearly, reaching a plateau at a Fn concentration consistent with one gelatin α-chain (100 kd) per Fn chain (220 kd). This stoichiometric titration provides the basis for a sensitive determination of Fn levels in plasma and other fluids. Interference caused by other proteins such as albumin, which has an affinity for the fluorescein moiety, could be minimized by addition of 1.0M NaCl which has no effect on the Fn-gelatin interaction.

W-AM-Po89 PURIFICATION, COMPOSITION AND VISUALIZATION OF A TETRODOTOXIN-BINDING GLYCOPROTEIN J. MILLER AND S. LEVINSON, UNIV. COLO. MED. SCHOOL, DENVER, CO., W. AGNEW, YALE SCHOOL MED., NEW HAVEN, CT., M. ELLISMAN, UNIV. CALIF. @ SAN DIEGO SCHOOL OF MED., LA JOLLA, CA. (INTR. BY M. NEVILLE)

We have purified the tetrodotoxin-binding component from E. electricus to homogeneity in near milligram quantities. The TTX-binding protein was found to consist only of a single polypeptide of 260,000 apparent molecular weight as determined by SDS-polyacrylamide gel electrophoresis. The protein stains positively with the periodate-Schiff reagent, demonstrating that the protein is glycosylated. No other polypeptides have been observed to copurify with this large component, raising the possibility that the component isolated may contain the ion pore and gating functions of the voltage-sensitive sodium channel.

We have determined the amino acid and carbohydrate compositions of the TTX-binding component and also have investigated its electrophoretic properties. The latter properties are unusual in that the protein possesses a very high electrophoretic free mobility and also has a large bandwidth on the polyacrylamide gels. The compositional analyses suggest that these anomalous electrophoretic characteristics are caused by acidic carbohydrate moities associated with the protein.

Electron micrographs of the protein reveal a rod-shaped molecule approximately 50 Å in diameter and 120 Å long. Either dimension would be sufficient to span the membrane bilayer.

W-AM-Po90 PROTON NMR OF INDOLE-EDTA, M. D. Kemple, IUPUI, Indpls., IN 46205, F. G. Prendergast, Mayo Med. School, Rochester, MN 55901, C. F. Meares, U. California, Davis, CA 95616, and B. D. Nageswara Rao, IUPUI, Indpls., IN 46205.

The ^{1}H NMR spectrum of 1-(3-methylene indole)-EDTA is examined at 470 Mhz. This molecule forms a 1:1 complex with di-and trivalent metal ions and, therefore, can serve as a model compound for the study of the interaction of these metal ions with tryptophan residues in proteins and for protein structure studies using lanthanide metal ions as shift reagents or relaxation reagents. The effects on the NMR spectrum of several paramagnetic rare earth ions (e.g. Yb^{3+}, Eu^{3+}, and Pr^{3+}) as well as diamagnetic La^{3+} will be described. For the Yb^{3+}-complex in particular, a number of resonances in the spectrum are observed to be in slow exchange on the NMR time scale. Shifts of indole proton resonances $\sim$0.7 ppm and of alphatic proton resonances greater than 8 ppm are observed upon binding of Yb^{3+}. In addition substantial broadening of the aliphatic proton resonances occurred. The measurements will be analyzed in terms of the magnetic interactions of the metal ions with the protons and related to the molecular geometry. Comparisons of these results will be made with similar measurements on a second EDTA derivative (benzyl-EDTA). (Supported in part by NSF Grants PCM 8022075 and PCM 7911492. The NMR measurements were performed at the Purdue University biochemical magnetic resonance facility supported by NIH Grant RR 01077.)

W-AM-Po91 SECONDARY STRUCTURE ANALYSIS AND ASSIGNMENTS IN PROTEINS, Salvatore V. Amato and Michael N. Liebman, Institute for Cancer Research, Philadelphia, Pa.

Since the solution of the first three-dimensional structure of a protein by X-ray crystallography, it has been of interest to identify elements of secondary structure and define their boundaries. Such efforts have attempted to permit the correlation of observations made in solution, from absorption spectroscopy, ORD and CD, with the structure in the "crystalline" state. Catalogs of structure, as stored in the Protein Data Bank, have been primarily obtained from the individual crystallographers, and therefore remain somewhat subjective. The most objective approach has been that of Levitt and Greer (J. Mol. Biol., 114, 181 (1977)), although this technique is involved in its application and limited in its type of structural definition.

We have developed a method based on distance matrix analysis, called the "neighborhood distance plot," which appears to be simple in concept yet provide a much broader capability for analyzing secondary structure. This technique allows the observation and delineation of standard forms of secondary structure (Ramachandran and Sasisekharan, Adv. Prot. Chem., 23, 283 (1968)); definition of appropriate boundaries; comparison and observation of more complex patterns of secondary structure which occur in more than one protein; presence of conformational repeats within a structure; definition of a secondary structural sequence; and a higher level of structural resolution for correlation with CD observations.

We have been developing techniques based on patterns recognition to identify new forms of secondary structure; using amino acid sequence comparison techniques to compare structural sequences; and extending our basis set for the interpretation of CD data.

W-AM-Po92 ORIENTATION AND INTERACTION ENERGY PROFILE STUDY OF PROTEINS, Michael N. Liebman, Salvatore V. Amato, and Thomas F. Kumosinski, Institute for Cancer Research and Eastern Regional Research Center, USDA, Philadelphia, Pa.

At present more than 130 protein structures have been examined at near atomic resolution by X-ray diffraction techniques. Of great interest have been attempts to correlate solution properties with the observed structural details. In many instances, these correlations have not proven to be successful as the patterns of structural organization appear to be more complex than previously imagined, i.e., presence and interaction of domains, quaternary structure, etc.

We have been interested in approaching this problem by deconvoluting the three-dimensional structure of atoms into a form which would more closely approximate the functional characteristics of the molecule. To do this we have been examining dipole alignments and interaction energies (i.e., dipole-dipole, charge-charge and charge-dipole).

In addition, we have used distance matrix analysis to contrast the functional aspects of molecular organization with the classical aspects of secondary, tertiary and quaternary structure. We have also examined the functional aspects of domain-domain interactions, organization around active site regions, surface versus interior regions and macromolecular recognition surfaces.

W-AM-Po93 SECONDARY STRUCTURE OF CRYSTALLINE NERVE GROWTH FACTOR AS DETERMINED BY RAMAN SPECTROSCOPY Jenny Gunning; Laboratory of Molecular Biology, Department of Crystallography, Birkbeck College, University of London, Malet Street, London WC1E 7HX, Robert Williams, and Bruce P. Gaber; Biomolecular Optics Section, Optical Probes Branch, Code 6510, Washington, D.C. 20375 USA

The intensity distribution of the amide I region of the Raman spectrum has been used to estimate the secondary structure of crystalline nerve growth factor (NGF). Using the method of Williams and Dunker[1], NGF is predicted to contain 9 $\pm$ 6% disordered helix and 50 $\pm$ 6% antiparallel beta-sheet. The primary structure[2] of NGF indicates there may exist a significant homology between NGF and insulin. On the contrary, the amide I band of NGF is substantially different from that of insulin, indicating that no structural homology is likely between the two proteins.

1) Williams, R. W. and Dunker, K. D. (1981), J. Molec. Biol. 152, 000-000.
2) Frazier, W. A., Angelliti, R. and Bradshaw, R. A., (1972) Science 176, 482-88.

W-AM-Po94 CHEMICAL AND SPECTROSCOPIC PROPERTIES OF THE PERIPHERAL SUBSTITUENTS OF HEME *a*. Julie Van Steelandt-Frentrup*, Patricia M. Callahan and Gerald T. Babcock. Department of Chemistry, Michigan State University, East Lansing, MI 48824.

The formyl group at the 8 position on the ring periphery of heme a confers unique optical properties on the basic porphyrin chromophore and is responsible for the red-shifted absorption spectrum of the heme a-containing protein, cytochrome oxidase. Moreover, the chemical properties of the formyl group and, to a lesser extent, the hydroxyl group on the 1' carbon at the ring 2 position are suggestive of possible mechanisms for both the redox potential heme-heme interaction observed in the protein and for the proton pumping function of cytochrome oxidase. To explore these possibilities, we have carried out an extensive characterization of the chemical and spectroscopic properties of these substituents. Our principal conclusions are the following: (1) The $-CH(OH)CH_2-$ substituent at the ring 2 position can be dehydrated easily to yield the unsaturated substituent. The optical spectrum of the ferric form of this species shows a slight blue-shift in both the α and Soret bands and the absorption intensity of the β-band increases relative to heme a. (2) The vibrational frequency of the formyl group is a strong function of iron spin and oxidation state and of solvent polarity. For low-spin species the carbonyl shifts by 30 cm^{-1} to lower frequency upon reduction; for high-spin species the corresponding shift is $\sim$10 cm^{-1}. The carbonyl vibration can be enhanced by laser excitation in resonance with either the heme a Soret or α-bands. (3) The formyl group is susceptible to facile chemical modification and, for example, imine, sulfite and oxime derivatives are easily formed. While these modifications have profound effects on the optical and Raman properties of the enzyme, the EPR spectra of the ferric complexes are essentially identical. (Supported by NIH Grant GM 25480.)

W-AM-Po95 MODELS FOR COMPOUNDS I OF PEROXIDASES: SPIN DENSITY INTERACTIONS WITH THE AXIAL LIGANDS. L.K. Hanson, I. Fujita, F.A. Walker and J. Fajer, Brookhaven National Laboratory, Upton, NY 11973.

An increasing body of evidence indicates that Compounds I, the two-electron oxidation transients in the enzymatic cycles of peroxidases and catalases, consist of ferryl species (Fe(IV)=O) coupled to cation radicals of the porphyrin macrocycles. In Compound I of horseradish peroxidase (HRP), electron abstraction from the porphyrin is postulated to occur from an a_{2u} molecular orbital on the basis of model studies and theoretical calculations (Hanson et al., JACS 103, 663 (1981)). ^{1}H, ^{14}N, and ^{17}O ENDOR results on HRP I support the ferryl a_{2u} π-cation assignment (Roberts et al., JBC 256, 2118 (1981); JACS, in press). Charge iterative extended Huckel calculations further predict that significant delocalization of unpaired spin density should also occur onto the histidine ligand of the HRP heme. Zinc tetraphenylporphyrin with a covalently linked pyridine was chosen as a model of an axially coordinated a_{2u} porphyrin radical. Although ligation of the metal by the pyridine induces only small optical and redox changes, ESR spectra establish that significant spin delocalization occurs onto the axial ligand, with a_N (pyridine) $\sim$4 MHz in agreement with the trend predicted by the calculations. Spin delocalization onto the axial ligands may provide additional stabilization for porphyrin radical intermediates and also suggests a mechanism for coupling the radical to its protein environment. Cytochrome c peroxidase may represent an extreme example of such an interaction in which its two-electron oxidation transient (Compound ES) would be preceded by a ferryl porphyrin π-cation followed by hopping of the hole on the cation to a nearby protein residue. (Work supported by the Division of Chemical Sciences, U.S. Department of Energy.)

W-AM-Po96 DIFFERENTIAL MELTING OF TROPOMYOSIN, A.L. JACOBSON, BIOCHEMISTRY DIVISION, DEPARTMENT OF CHEMISTRY, UNIVERSITY OF CALGARY, CALGARY, ALBERTA, CANADA, T2N 1N4.

Chicken cardiac tropomyosin has been studied by differential scanning calorimetry and by changes in extinction coefficient with temperature. Chicken cardiac tropomyosin unlike most of the cardiac tropomyosins is a pure β form of the protein (4SH/molecule). Changes at 278 nm indicate a conformational change occurs in the lower temperature range (~31°C) with both reduced and oxidized forms of the protein. An increase in hydrophobic interaction with temperature could account for the changes observed. Similar changes are not observed in the calorimetric study. Conformational changes are evident at higher temperatures in both calorimetric and UV measurements. Differential melting is observed. The reduced form has 2 major transitions while the oxidized form has 3 transitions in the higher temperature range.

W-AM-Po97 CRYSTALLIZATION OF THE TETRAMER OF HISTONES H3 and H4. Eaton Edward Lattman and Karen A. Magnus, Department of Biophysics, Johns Hopkins University School of Medicine, Baltimore, MD 21205, and Rufus Burlingame, Chris Hatch and Evangelos Moudrianakis, Department of Biology, The Johns Hopkins University, Baltimore, MD 21218.

Histones are now known to control the primary level of compaction of DNA in the eukaryotic chromosome. About 1-3/4 turns of DNA duplex is wound around the periphery of the histone octamer $(H2a\ H2b\ H3\ H4)_2$ to form a compact structure termed the nucleosome core particle. A core particle and its associated length of spacer DNA are termed a nucleosome. Evidence exists that the tetramer $(H3\ H4)_2$, a subassembly of the octamer, is the central component in organizing DNA into nucleosomes. Our attempts to crystallize various histone preparations have led to two types of $(H3\ H4)_2$ tetramer crystals. Type I was grown by vapor diffusion from whole tetramer using 6-12% w/v 6000 dalton P.E.G. These crystals are a maximum of .25 mm in length and .08 mm across. They show diffraction to 3.5 A resolution and are robust in the X-ray beam, but would be difficult to collect data from. Polyacrylamide gels of dissolved crystals and mother liquor reveal considerable proteolytic cleavage. Form II crystals are isomorphous to form I but are grown starting with a preparation of trypsinized tetramer. These grow rapidly to about .5 mm across but still have complex cleavage patterns. They belong to the space group $P6_1$ or $P6_5$ with a=b=80 and c=100 A.

W-AM-Po98 CHEMICAL MODIFICATIONS OF CYTOCHROME c OXIDASE. EFFECT OF SODIUM DODECYL SULFATE (SDS). E. Keyhani and J. Keyhani (Intr. by H. Davies), Inst. Biochem. Biophys., Univ. Tehran, Iran and Johnson Res. Fd., U. of Pa, Philadelphia, Pa 19104.

Incubation of beef heart cytochrome c oxidase with increasing concentrations of SDS produced: a) up to 0.1% SDS, no visible change in the α, γ and 830 nm absorption bands; b) over 1% SDS, a progressive decrease in the α, γ and 830 nm absorption bands (for 5% SDS, the absorptions were 35%, 45%, 0% of the value of the control, respectively). EPR spectroscopy showed a progressive decrease in the g3 signal with concomittant increase in the g6 signal. The copper signal (g=2) decreased progressively and was barely detectable at 10% SDS concentration. A new signal at g=2.45 was observed with SDS concentrations between 1.5 and 5%. Spectrophotometric determination of cytochrome c oxidase activity, using reduced cytochrome c, showed a stimulation of activity between 0.01%-0.1% SDS followed by progressive decrease of activity at higher concentrations. In contrast, polarographic determinations of activity, using ascorbate/TMPD as substrate, showed a progressive decrease in the enzymatic activity, without an early stimulation (Table I). The results in Table I are interpreted as evidence for distinct domains occupied by heme a and a3, being uncovered during denaturation by SDS treatment.

TABLE I (Activities in % control)

SDS (%)	0.01	0.05	0.10	0.20	0.30	0.40	0.50	1.00	2.00
Cyt. c	130	110	110	90	-	-	-	40	0
Asc./TMPD	-	80	50	30	17	8	0	0	0

W-AM-Po99 CHEMICAL MODIFICATIONS OF CYTOCHROME c OXIDASE : EFFECT OF MERCAPTOETHANOL. E. Keyhani, Inst. Biochem. Biophys., Univ. of Tehran, Tehran, Iran and Johnson Res. Fd., Univ. of Pennsylvania, Philadelphia, Pa 19104.

The stepwise addition of mercaptoethanol (MEtOH) to beef heart cytochrome c oxidase produced a progressive reduction of heme a (at 605 nm) and heme a3 (at 655 nm). The copper band (at 830 nm) remained unchanged up to 13 mM MEtOH, then became reduced, reaching full reduction at 130 mM MEtOH. In the presence of formate as ligand, after addition of MEtOH, heme a (at 605 nm) became progressively reduced, while copper remained unchanged up to 64 mM MEtOH, then decreased, reaching zero at 385 mM MEtOH. The 655 nm band remained virtually unchanged up to 250 mM MEtOH. However, reduction of the 655 nm band started after copper was 90% reduced. EPR spectra showed progressive decrease in the g3 and g2 signals with concomittant increase in the g6 signal. The reduced oxidase could not be reoxidized by addition of ferricyanide. Polarographic studies indicated that cytochrome c oxidase activity was decreased, reaching zero at 45 mM MEtOH. Approximately 80% of activity was restored upon 30 minutes incubation in GSSG-GSH mixture. Data suggest: a) the existence of some sort of coupling between the 830 nm copper and the 655 nm cytochrome a3, and b) ferricyanide cannot reoxidize heme a because of the S-S bond breakage and the change in the microenvironment of heme. The cytochrome c oxidase activity however can be restored by reformation of S-S bond and reestablishment of the microenvironment of heme and copper.

W-AM-Po100 A PREDICTED 3-D BACKBONE STRUCTURE FOR RIBITOL DEHYDROGENASE

Priscilla Wilkins Stevens and Tai Te Wu, Departments of Biochemistry & Molecular & Cell Biology and Engineering Sciences & Applied Mathematics, Northwestern University, Evanston, IL 60201.

A possible conformation for the backbone atoms of ribitol dehydrogenase, EC 1.1.1.56, (RDH) has been predicted. In the proposed structure, residues 16-124 form the coenzyme-binding domain; residues 125-247 fold as the catalytic domain; and the first 15 residues form an amino-terminal arm which may be important for tetramer formation. Within the family of NAD^+-linked dehydrogenases, positions of helices and β-strands which form the central core of the NAD^+-binding domain are well conserved. Hence, segments in RDH which may correspond to these structurally conserved elements were assigned atomic coordinates from equivalent features in lactate dehydrogenase (LDH). In accord with published experimental observations about RDH structure and function, Cys 126 and Ala 194 were positioned near the substrate-binding site, and possible catalytic residues were given orientations appropriate for a B-type dehydrogenase. This positioning in the LDH coordinate system of both the central core of the RDH NAD^+-binding domain and important RDH catalytic domain residues provided a framework onto which the remaining RDH segments were built. Since several research groups have crystallized RDH, an experimentally determined tertiary structure may be available in the near future for comparison with this predicted RDH conformation.

(Supported in part by NIH Grant 5-R01-GM21482 and NIH Contract N01-RR-8-2118 with the PROPHET computer system.)

W-AM-Po101 ULTRAVIOLET SPECTRA AND DIFFERENCE SPECTRA OF PROTEOGLYCAN SUBUNIT PREPARATIONS: ANOMALIES AND EFFECTED PERTURBATIONS. A. G. Beaudoin and D. Dziewiatkowski*, Dept. of Oral Biol. and Dental Research Institute, Univ. of Michigan, Ann Arbor, MI 48109.

Proteoglycan subunit (PGS), mol. wt. approximately 2 x 10^6 daltons, contains less than 10% protein. The remainder consists of glycosaminoglycan chains, attached to serine and threonine residues via glycosidic linkage, and shorter oligosaccharides. PGS of varying polydispersity was isolated from a rat chondrosarcoma. As evidenced by fine structure between 280nm-293nm, Guanidinium HCl (GdmCl) perturbation difference spectra at pH5.8 demonstrate that tyrosine/tryptophan exposure increases with increasing concentrations of GdmCl. Marked deviations in both Beer's and Lambert's Laws are observed in the absorption spectra. Particularly evident are: 1) an apparent blue shift (1cm path length, pH5.8) of the maximum from 228nm (8mg/ml) to 216nm (1.0 mg/ml); 2) a shift in the maximum from 231nm-235nm (2cm path length) to 225nm-228nm (1.0cm path length), all at 4mg/ml and pH5.8, and 3) a lack of correlation between path length or concentration and measured absorbance of the maximum. Although light scattering no doubt contributes to the phenomenon, it is suggested that fluorescence after low wavelength excitation may be involved. Significant differences in UV spectra also occur with change in pH. The fine structure of difference spectra, however, is obscured by a broad hyperchromic shift centered at 283nm. It is noted that PGS preparatory procedures influence the line shape of the absorbance spectrum and also of the pH difference spectrum. The results obtained particularly by GdmCl perturbation, suggest that spectral changes in the ultraviolet region may provide insight into conformational aspects of the "hyaluronate-binding region" of the protein core in PGS.

W-AM-Po102 SUBUNIT INTERACTIONS OF TRANSCARBOXYLASE: ANALYZING THE CIRCULAR DICHROISM FOR SECONDARY STRUCTURE, John P. Hennessey, Jr., W. Curtis Johnson, Jr., Chris Bahler, and Harland G. Wood, Department of Biochemistry and Biophysics, Oregon State University, Corvallis, Oregon 97331 and Department of Biochemistry, School of Medicine, Case Western Reserve University, Cleveland, Ohio 44106.

Orthogonal basis spectra are used to analyze the CD of transcarboxylase and its subunits for secondary structure. The method works well, even for the odd CD of the 1.3 S_H subunit. A change in the secondary structure of transcarboxylase resulting from quaternary interactions is monitored and traced to interactions among the six polypeptides that make up the 12 S_H subunit. The change is fully reversible and is not a result of the conditions used to dissociate the enzyme. It corresponds to an increase of 19% in α-helix, and a concomitant decrease of 8% in antiparallel β-sheet and 7% in random structure on association to form the hexameric 12 S_H subunit. (This work was supported by National Science Foundation grant PCM 80-21210 from the Biophysics Program, and by grants GM 22579 and AM 12245 from the National Institutes of Health.)

W-AM-Po103 THE THERMAL STABILITY OF OROSOMUCOID. T. L. Kirley and H. B. Halsall, Department of Chemistry, University of Cincinnati, Cincinnati, OH 45221.

The human serum glycoprotein orosomucoid (OMD) is widely reported as being extremely thermostable, up to temperatures of 100°C. We have found that the ligand binding properties of OMD fall off dramatically above about 46°C in phosphate-saline buffers pH 7.4, and that polymers which persist on cooling can be readily formed above this temperature. These observations indicate that progressive denaturing conformational events occur above 46°C. Confirmation was obtained principally by differential scanning calorimetry which yielded a single cooperative endotherm of T_m ~ 62°C and Δ H(transition) of 120 Kcal/mole. Comparison of the calorimetric and van't Hoff enthalpies indicated that this was not a two-state process. A domain structure could not be demonstrated for OMD with cyanogen bromide fragments, although some reannealing of these did occur. We suggest that the source of the apparent multistate behavior may lie in the existence of polypeptide variants, known to be present in OMD. OMD unpolymerized after heating shows reversible thermal denaturation behavior. Asialo OMD was more stable with T_m of 66°C and Δ H(trans) of 140 Kcal/mole. Polymers formed more rapidly and to a greater extent with asialo OMD than OMD at the same temperature, even though fewer molecules were in the denatured form. The T_m found correlates well with the empirical plot of Stellwagen and Wilgus relating T_m to molecular weight. We suggest that OMD does not show unusual thermostability, but merely a resistance to precipitation on heating, presumably due to the high carbohydrate content.

Supported by NIH Grant HD13207.

W-AM-Po104 FLUORESCENCE STUDIES OF CATALYTICALLY LINKED CONFORMATIONAL CHANGES IN RHODANESE. Paul Horowitz and Nick Criscimagna, Dept. of Biochemistry, The University of Texas Health Science Center at San Antonio, San Antonio, TX 78284.

One molecule of the apolar probe toluidinylnaphthalene sulfonate (TNS) binds to the enzyme rhodanese (EC 2.8.1.1) in each stable catalytic intermediate: free enzyme, E, or sulfur substituted enzyme, ES. TNS is a competitive inhibitor of the enzyme with an inhibition constant which was very similar to the fluorimetrically determined binding constant. The wavelength dependence (400-520 nm) of the life-time for TNS bound to rhodanese was determined at 20°C. At all wavelengths, the lifetimes measured by modulation were longer than those measured by phase. The value of M/cos ϕ increases with wavelength, but never becomes greater than 1. Controls using TNS in ethanol gave the expected lifetime of 7.8 nsec independent of wavelength or method of measurement. Acrylamide quenching of the native enzyme at 30°C gave Stern-Volmer (SV) plots which were convex to the abscissa indicating a significant contribution from static quenching. Analysis of the data gave SV constants that were numerically larger for E than for ES. The temperature dependence of the acrylamide quenching showed a thermally induced structural transition for the enzyme in the region of 25°C. At low temperatures the SV plots were approximately linear and the same for both E and ES. These data are interpreted in terms of a model in which the active site of rhodanese displays conformational heterogeneity because the enzyme active site is composed of contributions from two independent structural domains into which the single polypeptide chain is folded. Catalytically linked changes in the domain interactions are proposed which are associated with variations in rapid structural fluctuations of the protein. This research is supported by Welch grant AQ-723 and USPHS grant GM-25177.

W-AM-Po105 THE USE OF SMALL-ANGLE X-RAY SCATTERING FOR THE PREDICTION OF SEDIMENTATION COEFFICIENTS OF GLOBULAR PROTEINS. Helmut Pessen[1], Milton E. Noelken[2], and Thomas F. Kumosinski[1], [1]Eastern Regional Research Center, Agricultural Research Service, USDA, Philadelphia, PA 19118, and [2]Dept. of Biochemistry, University of Kansas Medical Center, Kansas City, KS 66103.

Renewed interest in the frictional properties of macromolecules and, more particularly, the contribution of hydration to the frictional coefficient, has emerged as a result of theoretical advances together with the availability of numerous X-ray crystallographic structures. Exact "shell-model calculations from three-dimensional structures (Teller, D. C., Swanson, E., and de Haën, C. (1979), Methods Enzymol. 61, 103-124) have shown agreement with experimental frictional coefficients, provided the model included a water molecule added to each charged group on the surface of a protein. We present a new semi-empirical procedure which relates solution small-angle X-ray scattering (SAXS) parameters to sedimentation coefficients. With this method, sedimentation coefficients were calculated for a set of 18 globular proteins of molecular weights ranging from 13,000 to 7,000,000; all were in excellent agreement with experimental values. Best results were obtained by using: (1), for the Stokes' radius in Svedberg's equation, the scattering volume V of the macromolecule instead of the commonly used partial specific volume $\bar{v}$ and (2), for the structural frictional ratio $(f/f_o)_s$, an axial ratio derived from R_GS/V instead of the usual $3V/(4\pi R_G^3)$ relationship, where R_G is the radius of gyration and S is the external surface of the molecule. This emphasizes the role of surface roughness as a determinant of the frictional coefficient. In addition, structural parameters from the X-ray crystallography can be compared with those from SAXS for a better insight into the hydration contribution to the frictional coefficient.

W-AM-Po106 PHOTOCHEMICAL PROBE OF PROTEIN INTERNAL FLEXIBILITY. A. A. Lamola and V. Pulito. Bell Laboratories, Murray Hill, NJ 07974.

The utility of the trans-stilbene to cis-stilbene photoisomerization reaction as a probe of the "flexibility" of the "heme pocket" of apomyoglobin is under investigation. It appears that trans-stilbene can be incorporated in the heme binding site of apomyoglobin, where, upon photoexcitation, it undergoes configurational isomerization. The primary process in the photoisomerization of unconstrained trans-stilbene is known to be a rapid twisting about the center carbon-carbon bond in the excited singlet state. The twisting rate is fast compared with both fluorescence and intersystem crossing, and so trans-stilbene exhibits a very low fluorescence quantum yield in solvents of low viscosity. An increased fluorescence yield and lower isomerization yield obtains when the solvent viscosity is increased. Because intersystem crossing is slow, there is a large range of viscosity wherein fluorescence yield and twisting rate are related in a simple way [Saltiel and D'Agostino, J. Amer. Chem. Soc., 94, 6445 (1972)]. Thus, the rate of a relatively well described geometry change (twisting) can be monitored rather easily by measurement of fluorescence intensity. The "flexible volume" required for twisting can be increased by incorporating substituents on the phenyl rings. We have observed that fluorescence from trans-stilbene bound to apomyoglobin is several-fold greater than that of stilbene in ethanol. The fluorescence yield increases additionally as sucrose or glycerol is added to the buffer.

W-AM-Po107 SECONDARY STRUCTURE PREDICTION BY LASER RAMAN SPECTROSCOPY Robert Williams, Code 6510, Naval Research Laboratory, Washington, D. C. 20375 USA

The Raman amide I bands of 11 crystalline proteins have been resolved into six components that correlate very strongly with the secondary structure of these proteins as estimated from x-ray diffraction data. These component bands, or reference spectra, can be fitted to the amide I spectra of other proteins to obtain predictions of secondary structure with a standard error of less than 6% for each parameter.

The parameters are: α-helix; disordered helix, such as found at the ends of helical segments and in 3_{10} helix; antiparallel beta-sheet; parallel beta-sheet; reverse turn; and undefined. This work extends earlier results[1], and is supported by a National Research Council Postdoctoral Fellowship. [1]R. W. Williams and A. K. Dunker, J. Mol. Biol, in press.

W-AM-Po108 THE 3 Å STRUCTURES OF IRON SUPEROXIDE DISMUTASES FROM E. COLI AND FROM P. OVALIS. William C. Stallings, Thomas B. Powers, Katherine A. Pattridge, James A. Fee and Martha L. Ludwig, Biophysics Research Division, The University of Michigan, Ann Arbor, Michigan 48109 and Dagmar R. Ponzi and Gregory A. Petsko, Chemistry Department, Massachusetts Institute of Technology, Cambridge, Massachusetts 02139.

The structures of iron superoxide dismutases from E. coli and from P. ovalis have been determined independently in two different laboratories using X-ray diffraction techniques. Both enzymes are dimers with an overall molecular weight of about 40,000 daltons. There is one iron site per subunit with an average Fe-Fe intersubunit separation of 17 Å. Determination of the non-crystallographic symmetry operation relating the two subunits has allowed us to use averaged maps as an aid in establishing the folding of the polypeptide chain. As predicted by circular dichroism measurements, helices are the dominant secondary structural features, and the iron dismutases are topologically unrelated to the Cu/Zn species. We will present a description of each structure and compare the independent interpretations of maps at 3 Å resolution.

W-AM-Po109 ESTIMATION OF VOLUME FLUCTUATION AGAINST "HYDROPHOBIC" FORCE. B.-K. Lee, DCRT/PSL, N.I.H., Bethesda, MD 20205 (Sponsored by R. J. Nossal)

The extent of volume fluctuation of globular protein molecules has been estimated using a model wherein (a) the protein is considered as a compressible sphere and (b) the mean potential energy, w, of the protein molecule as a function of its radius, r, is given by

$$w(r) = 4\pi\gamma r^2 \quad \text{when } r > r_o$$
$$= \infty \quad \text{when } r < r_o.$$

When the size of the protein is large compared to the fluctuation, the result is approximately given by $\delta V_{rms}/V = 3\ kT/(8\pi\gamma r^2)$. Using a value of 25 cal/mole/A^2 for γ, the computed values are compared with those estimated from the compressibility measurements (Gekko and Noguchi, J. Phys. Chem. (1979) 83:2706) for a number of proteins. The computed values are always larger than the experimental values by about 30% for larger proteins and by a factor of 2 or more for smaller ones. Although a different value of γ can improve the overall agreement with experimental values, the qualitative size dependence predicted by the theory is not discernible in the experimental data.

W-AM-Po110 OXYGEN AND ACRYLAMIDE FLUORESCENCE QUENCHING STUDIES WITH LIVER ALCOHOL DEHYDROGENASE USING STEADY STATE AND PHASE FLUOROMETRY. M. R. Eftink, Department of Chemistry, University of Mississippi, University, MS, 38677, and D. M. Jameson, Department of Biochemistry, University of Illinois, Urbana, IL, 61801.

The fluorescence lifetime of liver alcohol dehydrogenase (LADH) has been determined by phase fluorometry at various emission wavelengths and as a function of the concentration of the quencher acrylamide. Since acrylamide selectively quenches the fluorescence of the surface tryptophanyl residue, Trp 15 (Eftink and Selvidge, Biochemistry, in press), this allows the fluorescence lifetime of this residue and the buried residue, Trp 314, to be evaluated. Values of τ_{15} = 6.9 nsec and τ_{314} = 3.6 nsec are obtained, in qualitative agreement with lifetimes of these residues determined from fluorescence decay studies (Ross etal, Biochemistry 20, 4369-4377). The quenching of the fluorescence of LADH by oxygen (0 to 1500 psi) has also been studied. Quenching by oxygen results in a blue shift in the fluorescence of the protein and a downward curving Stern-Volmer plot. In the presence of 1M acrylamide (sufficient to quench almost all of the fluorescence of Trp 15, a linear Stern-Volmer plot for oxygen quenching is found, with a quenching constant of 3.5M^{-1}. This value can be assigned as the oxygen quenching constant of Trp 314. Taking into consideration the lifetime of 3.6 nsec for this residue, a rate constant for oxygen quenching of 1 x 10^9M^{-1}s^{-1} is obtained, the lowest reported for the oxygen quenching of a tryptophanyl residue in a protein. A lifetime Stern-Volmer plot has also been obtained for the oxygen quenching of LADH. Such a plot deviates somewhat from the intensity Stern-Volmer plot as predicted by simulations of the quenching of two component systems. (Supported by NSF Grant PCM 79-23031 and HEW PHS Grant GM 11223.)

W-AM-Po111 TRYPTOPHAN FLUORESCENCE AND PHOSPHORESCENCE OF HUMAN SEX-STERIOD BINDING PROTEIN
J.B.A. Ross[1], K.W. Rousslang[4], P.H. Petra[2], B.B. Olwin[3], P. McGarrah[4],
[1] Dept. Lab. Med., [2] Dept. Ob. Gyn., and [3] Dept. Pharm., Univ. Wash., Seattle, WA 98195; and
[4] Dept. Chem., Univ. Puget Sound, Tacoma, WA 98416.

Sex-steroid binding protein (SBP) from humans is a dimer containing about four tryptophan residues per molecule. SBP binds androgens in the serum and may transport steroid into target cells. Although its amino acid composition has been determined, nothing is known about the native structure of the molecule. Recent improvements in the isolation procedure makes it possible to carry out the physical characterization of SBP.

From our previous fluorescence, phosphorescence, and optical detection of magnetic resonance (ODMR) measurements of tryptophan in polypeptides and proteins, we have been able to distinguish a buried tryptophan from one that is relatively exposed to solvent.

The excited state parameters of the tryptophan(s) responsible for photoemission in SBP, saturated with steroid, are indicative of tryptophan in a buried or restricted environment. Thus the 0-0 band of phosphorescence is red-shifted (λ' = 413 nm) and the fluorescence is blue-shifted (λ' = 338 nm) compared with the model Gly-Trp-Gly (phosphorescence λ' = 408 nm, fluorescence λ' = 350 nm). Morever, on the basis of phosphorescence and fluorescence lifetimes, we can safely say that the emission is not monoexponential. The origins of the multiexponential emission kinetics, with regard to steroid binding, are being explored.

W-AM-Po112 FLUORESCENCE DECAY STUDIES OF ACID DENATURATION OF HORSE LIVER ALCOHOL DEHYDROGENASE. Dana Walbridge, Jay R. Knutson, and Ludwig Brand, The Johns Hopkins University, Baltimore, Maryland 21218.

Horse liver alcohol dehydrogenase (LADH) is known to undergo denaturation at acid pH as indicated by changes in UV absorption and fluorescence due to tryptophan, auramine O and TNS. We now show that the time course of acid denaturation (on the minute time scale) can be studied by means of nanosecond fluorometry. Native LADH exhibits bi-exponential fluorescence decay (τ_1 = 3.8 and τ_2 = 7.2 nsec). The short and long decay times are associated with the buried and exposed Trp residues respectively. A pulse fluorometer was modified so that a series of consecutive 40 sec. data collections could be obtained and stored in a computer. While the nanosecond decay is complex, we have found that it is useful to analyze the data in terms of a single exponential. The average fluorescence lifetime and amplitude both decreased during the course of denaturation. These results were compared with computer simulations for several quenching models. The simulated data (biexponential) were analyzed for an average monoexponential decay. Denaturation data were shown to be inconsistent with models describing equal static quenching, equal dynamic quenching and selective dynamic quenching of the long life-time component. The data is similar to the results predicted for a model with selective static quenching of the long component. The potential of utilizing rapid acquisition fluorescence decay data to investigate the kinetics of protein unfolding will be discussed. Supported by NIH grant No. GM11632. J.R.K. is a fellow of Pharmaceutical Manufacturers' Association Foundation.

W-AM-Po113 THE USE OF DIHYDROFOLATE REDUCTASE (FROM E. COLI) FOR INVESTIGATING THE EFFECTS OF SINGLE AMINO ACID SUBSTITUTIONS ON PROTEIN FOLDING AND STABILITY. C. R. Matthews, C. -P. D. Tu, N. A. Touchette, and K. -H. Lee, Penn State Univ., Depts. of Chemistry and Biochemistry, University Park, PA 16802

Dihydrofolate reductase (DHFR), Form I, from E. Coli strain RT500 was investigated as a system for studying the effects of single amino acid substitutions on protein folding and stability. The reversibility of urea-induced unfolding of DHFR Form I was monitored by recovery of activity and found to be greater than 95%. Measurements of $\Delta\varepsilon_{293}$ as a function of increasing urea concentration show changes consistent with exposure of tryptophan residues to solvent upon unfolding. The transition appears to follow a two-state model with a midpoint near 2.7M urea at pH 7.8, 25°C for Form I. Although the unfolding transition for an isozyme of DHFR, Form II, is similar to that of Form I, the midpoint is shifted to 2.9M urea. The increase in stability can be explained in terms of an additional electrostatic interaction in Form II which is absent in Form I. Sensitivity of this enzyme to trimethoprim permits a simple temperature-sensitive screening procedure to isolate mutants with altered thermal stability. Selection of a T_S mutant obtained by random mutagenisis with hydroxylamine yielded a strain with a substantially increased rate of heat inactivation of dihydrofolate reductase; sequencing studies are in progress. Thus, DHER appears to be an excellent candidate for a study of the effects of single amino acid substitutions on protein folding and stability. This work was supported by the National Science Foundation, PCM-8104495.

W-AM-Po114 ELECTROSTATIC CONTRIBUTIONS TO CONFORMATIONAL CHANGES IN BOVINE PANCREATIC TRYPSIN INHIBITOR. David G. Maskalick, Keith L. March, Richard D. England, and Frank R. N. Gurd, Department of Chemistry and Medical Sciences Program, Indiana University, Bloomington, IN 47405.

The modified Tanford-Kirkwood electrostatic theory has been employed to evaluate the pK values of all charge sites in the bovine basic pancreatic trypsin inhibitor (BPTI) as well as its total electrostatic free energy. The pK values for all the ionizable groups except the arginine residues have been determined by ^{13}C-NMR under conditions of nearly constant ionic strength in 0.10 M NaCl, at 41°C. General agreement is found between the computed and observed pK values. A localized, pH-dependent conformational change has been detected in ^{13}C-NMR spectra attributable to the formation of a salt bridge between the NH_2-terminal α-amino and the COOH-terminal α-carboxyl group. The cotitrations involved in this change can be distinguished from phenomena associated with other protonations or movements. The transition has been described hypothetically with a limited number and range of energetically facile bond rotations driven electrostatically and possibly augmented by hydrophobic contributions. The head-to-tail interaction contributes to the electrostatic stabilization of the molecule in the mid-range of pH, enhancing a net stabilization at neutral pH despite the substantial net positive charge borne by the protein under such conditions. (Supported by U.S. Public Health Service Research Grants HL-14680 and HL-05556.)

W-AM-Po115 HIGH FIELD PROTON NMR STUDIES OF INSULIN: ASSIGNMENT OF AROMATIC RESIDUE RESONANCES. D. Cheshnovsky*, L.J. Neuringer, R.A. Haberkorn*, MIT, Cambridge, MA; K.L. Williamson*, Mount Holyoke College, South Hadley, MA; S.G. Boxer, E. McCord*, Stanford University, Stanford, CA.

Insulin, a small protein hormone (MW ∿ 5750) consisting of two disulfide-linked polypeptide chains (A and B), plays a vital role in the regulation of mammalian carbodydrate, amino acid and fat metabolism. We report the first use of ^{1}H-NMR at 500 MHz and photo-CIDNP at 360 MHz to investigate dimeric zinc-free bovine insulin in solution. The insulin monomer contains 2 His, 3 Phe and 4 Tyr residues. In order to resolve and assign these proton resonances we performed the following experiments in deuterium oxide at various temperatures (5°C-60°C) and pH values (2.1-3.0): spin-decoupling, Carr-Purcell, photo-CIDNP and 2 dimensional J-resolved and auto-correlated spectroscopy. Experiments were also carried out in 7 M urea. In addition, desoctapeptide (B23-B30) insulin which lacks B24 Phe, B25 Phe, B26 Tyr was useful for assigning the B26 Tyr and B1 Phe resonances, the latter being comprised of two triplets and one doublet. Photo-CIDNP experiments identified A14 Tyr which is known to reside on the surface of the insulin dimer and to be exposed to solvent. At 500 MHz and T = 58°C the resonances from the C(2) and C(4) imidazole protons of B5 His and B10 His can be resolved and assigned. It appears that the environments of B5 His in molecule I and molecule II of the dimer are the same, with the same being true for B10 His. The T_2 relaxation times of the C(2) and C(4) protons of B10 His are found to be shorter than those of B5 His. This is plausible because B5 His is located in a region of the protein which is extended and conformationally mobile whereas B10 His is part of the α-helical portion of the B-chain and is thus situated in a more rigid environment. Work supported by the NIH and NSF.

W-AM-Po116 PHYSICO-CHEMICAL STUDIES ON THE Ca^{2+} AND K^{+} INDUCED CONFORMATIONAL CHANGES IN BOVINE BRAIN S-100b PROTEIN. R.S. Mani* and C.M. Kay. MRC Group in Protein Structure and Function, University of Alberta, Edmonton, Alberta T6G 2H7, Canada.

The brain specific S-100 protein is a mixture of two components, S-100a and S-100b, with a subunit composition of αβ or β_2, respectively. S-100b, isolated using hydroxylapatite chromatography in its final purification, is homogeneous by the criteria of gel electrophoresis in the absence and presence of SDS and ultracentrifuge studies. Molecular weight studies by both sedimentation equilibrium in 6 M guanidine-HCl and 15% SDS gels indicated the subunit molecular weight to be 10,500 and since a molecular weight of 21,000 was obtained in native solvents, the protein exists as a dimer in benign medium. The two subunits are held together by noncovalent forces. The S-100b protein undergoes a conformational change upon binding calcium, as revealed by UV difference spectroscopy and CD studies in the aromatic and far UV range. Far UV CD studies indicated the apparent helical content to drop from ∿58 to 52% in the presence of Ca^{2+}. The effect of K^{+} on the protein was antagonistic to Ca^{2+} and the protein's affinity for calcium was lowered by the presence of K^{+}. The conformational state of the protein is very much dependent upon the metal ions (Ca^{2+},K^{+}) present, suggesting that changing conformation may be the way S-100 affects some of the ionic parameters in the brain such as fluxes and local concentration of ions. Fluorescence studies indicate the presence of an abnormal tyrosine in the protein with the emission maximum centered at 330 nm when the protein is excited at 280 nm.

W-AM-Po117 PROTEIN CONFORMATION FROM ELECTRON SPIN RELAXATION DATA. J. P. ALLEN, J. T. Colvin, & H. J. Stapleton, Physics. Dept., Univ. of Illinois, Urbana, IL 61801.

Electron spin relaxation data from five low spin ferric proteins are presented as evidence that the fractal model of Stapleton et. al. (1) provides an accurate description of electron spin relaxation rates in these biopolymers. This model relates protein structure, as characterized by a fractal dimension d (2), and the density of vibrational states $\rho(\omega)$, which varies as $\omega^{**}(d-1)$, to the temperature dependence of the Raman relaxation rate, which then varies as $T^{**}(3+2d)$. X-ray data from 17 protein structures show that they are characterized by non-integral values of d which range from about 4/3 to 7/4, thus bracketing the 5/3 value of d associated with a self-avoiding random walk in three dimensional space. In simplistic terms, the fractal dimension d could be associated with the inverse of the Flory constant, which relates the radius of gyration of a polymer to the number of monomers in the polymer chain. Among the relaxation data we present are the results of three different research groups on ferricytochrome c and ferredoxin. The d values for ferricytochrome c are 1.66±0.05 and 1.67±0.03 using x-ray data and relaxation data respectively. Similar results for ferredoxin are 1.34±0.05 and 1.34±0.06. Although the fractal dimensionality is but a single structural parameter, it is nevertheless a useful indicator of protein conformation because it provides a quantitative measure of the degree to which polypeptide chain fills the space in which it resides. This work was supported by the U. S. PHS under NIH Grant GM24488.

(1) H. J. Stapleton et. al. Phys. Rev. Lett. 45, 1456 (1980).
(2) B. B. Mandelbrot, "Fractals; Form, Chance, and Dimension", (Freeman, San Francisco 1977).

W-AM-Po118 EQUILIBRIUM FOLDING-UNFOLDING PATHWAYS IN PROTEINS. S. Miyazawa and R. L. Jernigan, (Intr. by D. Torchia) Laboratory of Mathematical Biology, DCBD, NCI, NIH, Bethesda, MD 20205

Protein conformations are generated with a "Non-Interacting Local Structure Model"; each residue is assumed to take either the native or random coil state, and a protein conformation is regarded to consist of alternating sequences of random coil and native parts. Statistical weights of protein conformations are taken to consist of two parts: from intra-residue and inter-residue interactions. An intra-residue statistical weight for each residue in the native state is taken to be proportional to the empirical frequency of the native (ϕ, ψ). Inter-residue energies are assumed to be proportional simply to the numbers of contacts in the native parts. For the purpose of describing most probable pathways, the number of native residues is employed as a simple one-dimensional representation of a folding coordinate. The most probable conformations are determined by considering all possible combinations of native and random coil parts at each point along this coordinate. This provides a description of the conformational characteristics of relatively rare intermediates on the folding pathway. Such folding-unfolding pathways have been constructed by connecting most probable conformations in order according to the total number of native residues. For each protein, free energies and the probabilities of residues in the native state at each stage of folding are calculated for a wide range of contact energy. The method requires only a simple matrix calculation. The free energies depend strongly on the value of the contact energy; however the most probable conformations remain relatively invariant, indicating that the pathways are less sensitive to its value. Proteins studied include lysozyme, myoglobin, ribonuclease A and trypsin inhibitor. Results for the last molecule are similar to those obtained in a Monte Carlo simulation with a more detailed model.

W-AM-Po119 SECONDARY STRUCTURE OF COLLAGEN PROPEPTIDES AND TELOPEPTIDES. T.E. Doering, E.F. Eikenberry, B.R. Olsen, P.P. Fietzek, and B. Brodsky. Dept. of Biochemistry, CMDNJ-Rutgers Medical School, Piscataway, N.J. 08854

Collagen in higher vertebrates consists of a family of closely related genetic types. The best characterized members - Types I, II, and III - have a central triple-helical region with small non-helical peptides (telopeptides) at each end. Type I collagen contains two types of chains, $\alpha1$(I) and $\alpha2$, whereas Types II and III each contain only one chain type, $\alpha1$(II) and $\alpha1$(III) respectively. These collagens are synthesized in a precursor form with large globular propeptides at each end, which are specifically cleaved during the processing of the molecules into fibrils. To gain insight into the conformations and functions of these non-triple-helical domains, we calculated predicted secondary structures of the telopeptides and propeptides of different genetic types from their amino acid sequences. The N-telopeptides of $\alpha1$(I), $\alpha2$, $\alpha1$(II), and $\alpha1$(III) chains were found to differ considerably in secondary structure, but the C-telopeptide domains had similar conformations, as did the N-propeptides of $\alpha1$(I) and $\alpha1$(III) chains. The structures of the C-propeptides of both chains of Type I collagen were nearly identical, whereas the region of the $\alpha1$(II) C-propeptide that is available did not show similar features. Processes which all collagens undergo include triple-helix formation, secretion from the cell, and fibril formation. Our results suggest that the C-telopeptide and N-propeptide domains are involved in such common functions. On the contrary, the conformations of the N-telopeptides and C-propeptides suggest that these regions are involved in functions which require discrimination between genetic types, such as chain selection for triple-helix formation and regulatory functions.

W-AM-Po120 A VISCOSITY DEPENDENT SUBMILLISECOND RELAXATION OF RIBONUCLEASE A IN THE THERMAL UNFOLDING ZONE. Tian Yow Tsong, Department of Physiological Chemistry, Johns Hopkins University School of Medicine, Baltimore, Maryland 21205

Previous studies monitoring tyrosine absorption changes have failed to detect rapid unfolding reactions of ribonuclease A (RNase) at pH 7 by the temperature jump method, although they (in 50 ms time range) have been observed by the stopped-flow pH jump in both unfolding (pH 7→2) and refolding (pH 2→7) directions. By coupling the unfolding reaction to the color change of a colorimetric indicator, phenol red, in an unbuffered protein solution, at least three relaxations from submilliseconds to seconds have now been resolved with a 4 degree T-jump over the range 10° to 80°, at pH 7. The fast reaction (τ_f=0.9 ms at 25°) detected a proton uptake with a pK_a of 6 was observable in the entire folding-unfolding zone, and was found to depend strongly on the microscopic viscosity of the solvents. The other two slower relaxations also detected a proton uptake, but with a pK_a of about 8, were independent of the solvent viscosity and have similar relaxation times for the folding-unfolding of RNase monitored by the tyrosine absorption, under similar experimental conditions (τ_2~80 ms, τ_1~10 s at pH 7, 25°). All three reactions were present even at 25° or at 80°, i.e. much below, or high above the thermal melting temperature (61°). Two possible interpretations are given. 1) If at 25°, all of the RNase molecules are in the folded state the τ_f reaction could reflect solvent permeation into the interior of protein structure. 2) Conversely, if a small fraction of protein molecules exist in the unfolded form even at 25°, τ_f reaction could have detected an early step in protein folding. The diffusion-collision-association of structure embryos in a peptide chain has been predicted to depend on solvent visosity. (NSF Grant PCM8109630)

W-AM-Po121 CELL-FREE SYNTHESIS OF HUMAN APO A-I AND APO E. D.G. Ross, V.I. Zannis, D.M. Kurnit, and J.L. Breslow, Metabolism Division, Children's Hospital Medical Center and Dept. of Pediatrics, Harvard Medical School, Boston, MA 02115.

Total mRNA isolated from fetal human liver was translated in vitro in the presence of ^{35}S methionine using a rabbit reticulocyte cell-free translation system. The cell-free translation mixture was immunoprecipitated with antibodies to apo A-I and/or apo E and the immunoprecipitate was analyzed by two-dimensional polyacrylamide gel electrophoresis and autoradiography. Antibody to apo A-I immunoprecipitated two proteins which have a slightly higher MW and a more basic isoelectric point than the major apo A-I isoprotein seen in plasma. These proteins, presumed to be apo A-I precursors, are approximately 1% of the total ^{35}S methionine-labeled proteins translated in vitro. A mixture of antibodies to apo A-I and apo E immunoprecipitated not only the putative apo A-I precursors, but also two other proteins which overlapped on two-dimensional gels with the asialo forms of plasma apo E (apo E2 and apo E3). The immunoprecipitated apo E was less abundant than the apo A-I. These experiments suggest that: (a) There are two translation products of apo A-I, (b) Apo A-I is synthesized as a high MW precursor, which suggests that the primary translation product of apo A-I contains a leader peptide sequence. This sequence may be involved in apo A-I secretion, (c) The primary translation product of apo E appears to have the same MW and isoelectric point as plasma apo E, (d) Fetal human liver is a good source of mRNA coding for apo A-I and apo E. The abundance of these mRNA's in liver may facilitate cloning of the human apo A-I and apo E genes.

W-AM-Po122 STELLACYANIN: STRUCTURE OF THE METAL BINDING SITE AS DETERMINED BY X-RAY ABSORPTION SPECTROSCOPY. J. Peisach, L. Powers, W. E. Blumberg, and B. Chance. *Bell Laboratories, Murray Hill, NJ 07974, Departments of Molecular Pharmacology and Molecular Biology, Albert Einstein College of Medicine, Bronx, NY 10461, and Johnson Research Foundation, University of Pennsylvania Medical School, Philadelphia, PA 19104.*

Stellacyanin is a mucoprotein of molecular weight ≃20,000D obtained from *Rhus vernicifera*, the Japanese lac tree. The protein contains one copper atom in a blue or type 1 site. As the metal ion can exist in both the Cu(II) and Cu(I) redox states, the protein may function as an electron carrier, although the rate of reduction of the native enzyme by dithionite is exceedingly slow. The metal binding site in plastocyanin, another blue copper protein, [P. M. Colman *et al.*, 1978, **Nature 272:** 319-324.] contains one cysteinyl, one methionyl, and two imidazoyl residues, but the exact analog of this site cannot exist in stellacyanin as it contains no methionine. The copper coordination in the latter protein has been studied by x-ray edge absorption spectroscopy and extended x-ray absorption fine structure (EXAFS) analysis. A new, very conservative data analysis procedure has been introduced. The results suggest that there are two nitrogen atoms in the first coordination shell of the oxidized protein and one in the reduced protein. In both oxidation states these N atoms have normal Cu-N distances, 1.95Å. In both states of the protein there are either one or two sulfur atoms coordinating the copper, the exact number being indeterminable from the present data. In the oxidized state the Cu-S distance is intermediate between the short type found in plastocyanin and the normal type found in near tetragonal copper model compounds. If the x-ray experiments are carried out at temperatures above -140°C, radiation damage of the protein occurs. At room temperature the oxidized protein is modified by radiation in the synchrotron x-ray beam at a rate of 0.25%/sec.

W-AM-Po123 ASSEMBLY OF RIBULOSE BISPHOSPHATE CARBOXYLASE

Mark Bloom, Patrice Milos, Maureen Monroe, and Harry Roy
Rensselaer Polytechnic Institute, Troy, New York 12181.

Ribulose bisphosphate carboxylase carries out the CO_2 fixation step in the Calvin cycle. This enzyme consists of eight catalytic ("large") subunits (Mr = 55 kD) and eight ("small") subunits (Mr = 14 kD) and has a sedimentation coefficient of 18S. Large subunits of this enzyme, labeled in vivo or in vitro, can be recovered from intact chloroplasts in two different complexes with sedimentation coefficients of 7S and 29S. Upon prolonged illumination of the chloroplasts, newly synthesized large subunits accumulate in the 18S ribulose bisphosphate carboxylase molecule and disappear from both the 7S and 29S complexes. The loss of radioactivity from either the 7S or the 29S complex is sufficient to account for the increase in radioactivity in the 18S enzyme. Each complex is therefore a possible intermediate in the assembly of ribulose bisphosphate carboxylase. The 29S complex consists of an undetermined number of 60 kD polypeptide subunits ("large subunit binding protein") and a trace amount of 55 kD large subunits, (probably less than one 55 kD subunit per 29S complex). More than half the newly synthesized large subunits associate with this complex. It is considered that this aggregate of the 60 kD "large subunit binding protein" may represent a catalytic assembly factor similar to those described in bacteriophage assembly.

W-AM-Po124 CALCIUM DEPENDENT PHENOTHIAZINE BINDING PROTEINS FROM THE OPTIC LOBES OF THE SQUID LOLIGO PAELEI. J.F. Head, S. Spielberg and B. Kaminer. Dept. of Physiology, Boston University School of Medicine, Boston, MA 02118.

The antipsychotic phenothiazine drugs have been used extensively as probes of calmodulin function based on their ability to bind to calmodulin in the presence of calcium and to block its action as a calcium dependent regulator. The interaction of calmodulin with these drugs has also been employed as the basis for affinity chromatographic procedures for the specific isolation of calmodulin from various tissue sources. In our studies of squid optic lobe we have found that calmodulin is not the only protein able to bind to phenothiazines. Two squid proteins bind to Fluphenazine-Sepharose in a calcium dependent manner. These proteins can be separated from one another by ion exchange chromatography on DEAE cellulose. One protein apparently corresponds to calmodulin, based on its amino acid composition, including a single residue of trimethyllysine, its electrophoretic mobility and its ability to activate calmodulin dependent phosphodiesterase. The second protein has the same molecular weight as calmodulin, as determined by SDS gel electrophoresis, but migrates separately on alkaline urea gels, has a distinct amino acid composition, with no trimethyllysine, and does not activate calmodulin dependent phosphodiesterase. Both proteins are able to bind to ^{3}H-chlorpromazine in the presence of calcium. These studies suggest that caution should be used in the employment of phenothiazines as calmodulin-specific probes or affinity ligands in in-vitro studies and may indicate that proteins other than calmodulin in neural tissue could act as targets for these antipyschotic drugs. (Supported by NIH grant AM 18207 and NSF grant PCM 7904600.)

W-AM-Po125 A PHENOTHIAZINE BINDING FRAGMENT FROM BOVINE BRAIN CALMODULIN. J.F. Head, H.R. Masure and B. Kaminer. Department of Physiology, Boston University School of Medicine, Boston, MA 02118.

The antipsychotic phenothiazine drugs bind to the intracellular activator protein calmodulin in a calcium dependent manner and block the activation of various calmodulin dependent enzyme systems. In our present studies we aim to characterize the phenothiazine-calmodulin interaction sites to improve our understanding of the mode of action of these drugs. As a preliminary in this investigation we have cleaved bovine brain calmodulin with cyanogen bromide and have employed affinity chromatography on fluphenazine-Sepharose to isolate any phenothiazine binding fragments. Using this procedure we have isolated a single peptide which binds to the Fluphenazine resin in a calcium dependent manner. Based on the size of the fragment and its amino acid composition we tentatively designate it as corresponding to the region of the molecule extending from residue 77-124, resulting from incomplete cleavage at Met_{109}-Thr_{110}. This section of calmodulin includes all of calcium binding domain 3, Tyr 99 the sole His (107) and the characteristic single trimethylsine (115) of calmodulin.

The phenothiazine binding fragment has no effect on the activity of bovine brain calmodulin dependent phosphodiesterase.

(Supported by NIH grant AM 18207 and NSF grant PCM 7904600.)

W-AM-Po126 SALT DEPENDENCE OF HYDROGEN EXCHANGE KINETICS OF BOVINE PANCREATIC TRYPSIN INHIBITOR. Erik Tüchsen* and Clare Woodward. Dept. of Biochemistry, Univ. of Minnesota, St. Paul, MN 55108.

The effects of neutral and denaturing salts on the total tritium-hydrogen exchange kinetics of bovine pancreatic trypsin inhibitor (BPTI) have been measured. The data are gathered for the change with time in the number of H unexchanged with solvent isotope per molecule of protein. The total exchange kinetics represent the average kinetics of all labile protons measured simultaneously from a uniformly tritium-labelled protein. The protons exchanging in the experimental time range (2 min-36 hr) are peptide NH's. In native BPTI, pH 6.5, the temperature coefficients for exchange rates differ with the concentration and with the type of salt. Over the temperature range 20-35°C, the apparent activation energies are 17, 21 and 24 kcal/mol (±10%) in 0.3 M KCl, 3 M KCl and 3 M guanidine·HCl, respectively. At 20°, the exchange curves in 0.3 M KCl and in 3 M guanidine·HCl are coincident, but at ~35°, exchange is markedly slower in 0.3 M KCl than in 3 M guanidine·HCl. At all temperatures the exchange kinetics in 3 M KCl is slower than in the other two salt solutions. Analogous experiments with fully reduced and alkylated BPTI, in which the three disulfide bonds are irreversibly cleaved, measure the contributions to exchange in native BPTI arising from the salt dependence of the chemical exchange step. This allows an estimate of the salt effect on the rate limiting conformational process in the folded state.

W-AM-Po127 MACROMOLECULAR SURFACES, VOLUMES, CHANNELS AND VOIDS, Thomas F. Kumosinski, Salvatore V. Amato, Michael N. Liebman, Eastern Regional Research Center, USDA, and Institute for Cancer Research, Philadelphia, Pa.

X-ray crystallography has shown that the three-dimensional structure of macromolecules exhibits highly convoluted surfaces, clefts and channels. These features are preserved through evolution and appear related to macromolecular organization and function. Molecular surfaces have been examined to determine accessible surface areas and molecular volumes. Individual investigators tend to emphasize different characteristics of the structure, particularly concerning solvent-protein interfaces. The mean volume of the molecular interior as well as variations in density appear dependent upon the sampling techniques used in the calculations.

We have developed an algorithm which appears to be independent of sampling parameters in its consistency. It has revealed that the localized density variations result from significant voids within the molecular interior. These voids do not necessarily connect to the molecular surface in the static model of the crystal structure.

We have examined a series of protein structures, under varying conditions and among several families of structure to catalog the presence of these voids and channels. This has been done to better correlate small angle X-ray scattering observations on these macromolecules. In addition, we have examined the location of these voids to determine their relevance to domain structures, active site regions and have mapped the electrostatic potential in the surrounding region. Analysis and comparison has also been carried out using computer graphics.

W-AM-Po128 THE CHEMICAL BOND ENERGY IN INTERACTING PROTEIN SYSTEMS · Paul W. Chun and James Q. Oeswein. Department of Biochem. and Mol Biol., Univ. of Fla., Gainesville, Fla. 32610.

The chemical bond energies at 0°K of four self-interacting protein systems — α-chymotrypsin, S-CAM apolipoprotein A-II, bovine liver L-glutamate dehydrogenase, and glucagon — were determined to be 33.6 ± 0.86, 50.56 ± 1.89, 26.8 ± 1.29, and 29.8 ± 18.96 kilocalories per mole, to the best approximation, by extrapolation from experimentally determined values of $\Delta G^0(T)$ at 278° to 317°K. Analysis of the Planck-Benzinger thermal work function, $\Delta W^0(T)$, as applied to these interacting protein systems, indicates that it is an expression of the heat available from the formation of chemical bonds between associating units, and is equal to the heat absorbed and the work done when such chemical bonds are broken. Thus $\Delta W^0(T)$ represents a driving energy potentially available for interacting protein systems and is a determinant in maintaining the chemical equilibrium in these interacting systems. (This work was supported by NSF Grant PCM 76-04367 and in part by PCM 79-25683.)

W-AM-Po129 TROPONIN T-TROPOMYOSIN INTERACTION. P.C.S. Chong and R.S. Hodges, Department of Biochemistry and Medical Research Council Group in Protein Structure and Function, University of Alberta, Edmonton, Alberta, Canada T6G 2H7.

Recently three different studies have indirectly indicated that troponin T (TnT) is in the vicinity of cysteine 190 or 1/3 of the distance from the COOH-terminal end of α-tropomyosin (Tm). In order to locate the actual region of TnT in the close proximity to Tm, under physiological conditions (the presence and absence of Ca^{2+}), the binding of S-carboxamidomethylated skeletal troponin (CM-Tn) was photochemically crosslinked to α-Tm which was labelled with a heterobifunctional photoaffinity probe, N-(4-azidobenzoyl-^{3}H-glycyl)-S-(2-thiopyridyl)-cysteine (AGTC) at cysteine 190. The covalently linked complex (CM-Tn-AGC-Tm) was isolated by hydroxylapatite chromatography in the presence of reducing agent which cleaved the disulfide bond between AGC-Tm and CM-Tn. The radiolabelled CM-Tn was separated into its individual components by DEAE-Sephadex chromatography in 6 M urea, EGTA and DTT. Radioactive measurements indicated that only TnT was labelled. Chymotryptic digestion of radiolabelled CM-Tn indicated that the C-terminal fragment of TnT (T_2, residues 159-259) was the only component radiolabelled. These results suggest that in the presence and absence of Ca^{2+} TnT binds to Tm in such a way that the C-terminal region (residues 159-259) is within 14 Å of Cys 190 in Tm. These results are in agreement with fragment binding and fluorescence studies. (Supported by MRC).

W-AM-Po130 PICOSECOND SPECTROSCOPY OF CU(II) CYTOCHROME C. A. Reynolds*, K.D. Straub** and P.M. Rentzipis*. *Bell Labs, Murray Hill, N.J., **VA Med. Center and Univ. of Ark. for Med. Sciences, Little Rock, Ark.

In order to study the energy dissipation pathways in electronically excited hemoproteins, we have investigated the picosecond relaxation of Cu(II) cytochrome c. Upon excitation at 355 nm the Soret bands and the α and β bands undergo bleaching (depletion of ground state) while the ranges between 440 and 500 nm as well as at > 590 nm have increases in optical density due to absorbtion by the excited states. At neutral pH the Soret band has a strong peak at 420 nm and a weaker one at 404 nm. The 420 nm peak bleaches upon excitation and returns to ground state in approximately 10 psec while the 404 nm bleaching lasts longer than 1 nsec. The bleaching of the α and β bands and the absorbtion of the excited state have lifetimes similar to the 420 nm bleaching. At extreme pH values of 2.5 and 13.0 the Cu(II) cytochrome c has only a 404 nm peak with very little absorbtion at 420 nm. The bleaching at 404 nm lasts longer than 1 nsec. The bleaching of the α and β bands as well as the excited state absorbtion also last longer than 1 nsec. These relaxation kinetics are significantly different from two observable decay rates of Cu(II) protoporphyrin IX dimethyl ester in benzene (450 psec and > 1 nsec). Since the visible absorbtion spectrum of the ground state Cu(II) cytochrome c at neutral pH demonstrates a broad low absorbtion band at 683 nm, it is likely that in addition to the tridoublet and tripquartet states, a charge transfer state provides relaxation pathways for the electronically excited Cu(II) cytochrome c. Similar data will be presented for Fe(II) cytochrome c.

W-AM-Po131 INTERACTION OF INHIBITORS WITH LOW-TEMPERATURE OXYGEN INTERMEDIATES OF CYTOCHROME OXIDASE F.Yang,C.Kumar,K.DeFonseka,B.Chance, Johnson Res.Fnd,U. of PA,Philadelphia,PA.

In an attempt to chemically characterize the coordination status of Fe^{3+} in the Fe-Cu active site in the low-temperature intermediates of the reaction of O_2 with cytochrome oxidase, we have studied the reaction of respiratory inhibitors with these intermediates in mitochondria and in the purified enzyme. The methods used are optical and epr spectroscopy. Reduced CO-bound cytochrome oxidase is cooled to -20°C in the dark, an appropriate quantity of inhibitor is added, the solution is oxygenated and freeze-trapped at -78°C. The sample is subsequently photolyzed at a desired low temperature (-85° to -100° range) and optical and epr changes are followed with time. The inhibitors used were azide, cyanide, fluoride, and sulfide. All these seem to interact rapidly with the cytochrome oxidase intermediates(B_1,B_2) at these temperatures. The main features seen are (a) new charge transfer bands(metal to ligand) in the 600-700nm region; (b) different extents of heme oxidation depending on the inhibitor; and (c) new epr signals; e.g., near g = 3.1 with azide due to metal inhibitor complexes. The reaction of these inhibitors with the heme centers at such low temperatures under conditions of significant oxidation of [$\underline{a}_3$, $\underline{Cu}_{\underline{a}_3}$] due to electron transfer to oxygen demonstrates competition between the inhibitor and the cysteinyl sulfur for the ferric iron available following peroxide reduction to water.

(1)Powers et al, Biophys.Jour 34:465-498,1981.

Supported by NIH grants GM28308,HL-SCOR-15061,SSRL Project 423B(DDR,DOE,NSF).

W-AM-Po132 CYTOCHROME $\underline{c}$-CYTOCHROME OXIDASE INTERACTIONS AT LOW TEMPERATURES. C. Kumar and B. Chance Johnson Res. Foundation, Univ. of Penna. Phila,PA. Introduced by Alan Waring

Continuing our past studies on the above topic (1) we present significant new results here that suggest that cytochrome $\underline{c}$-cytochrome oxidase interactions significantly affect the heme-heme interactions in cytochrome oxidase at low temperatures. Reduced, CO bound normal (+$\underline{c}$) and cytochrome $\underline{c}$-depleted (-$\underline{c}$) beef heart mitochondria, suspended in 30% ethylene glycol buffer pH 7.4, were oxygenated by stirring at 253°K, frozen and flash photolyzed at 77°K and incubated (from 1 to 15 min) at temperatures ranging from 173° to 213°K. Periodic EPR measurements give the initial rate of oxidation of $\underline{Cu}_{\underline{a}}$ and heme $\underline{a}$, cytochrome $\underline{c}$ ($\underline{c}$) and the Fe-S proteins.

At 173°K, there is very little cytochrome $\underline{c}$ oxidation (<3%) and heme $\underline{a}$ oxidation is significantly more (∿70% in 15 min) in +$\underline{c}$ than in -$\underline{c}$ (∿55% in 15 min). At 213°K, however, in -$\underline{c}$, heme $\underline{a}$ oxidation is more rapid (∿75% in 15 min) than in +$\underline{c}$ (∿55% in 15 min). +$\underline{c}$ also shows significant $\underline{c}$ oxidation (∿12 mole% of heme $\underline{a}$ present) at 213°K.

At 173°K,+$\underline{c}$ shows greater electron transfer between heme $\underline{a}$ and $\underline{a}_3$, leading to higher heme $\underline{a}$ oxidation. At 213°K, the lower extent of initial heme $\underline{a}$ oxidation is due to rapid $\underline{c}$ to heme $\underline{a}$ electron transfer at that temperature. A model of cytochrome $\underline{c}$-cytochrome oxidase interactions consistent with cytochrome $\underline{c}$ facilitation of heme $\underline{a}$ to $\underline{a}_3$ electron transfer(as indicated by the 213°K results)will be presented.

(1)B.Chance et al. Biochim.Biophys.Acta.503:37-55,1978.

Supported by NIH grants 27308 and HL-SCOR-15061 and by SSRL Project 423B(NSF,DDR,DOE).

W-AM-Po133 MOBILITY OF CYTOCHROME c ON MITOCHONDRIAL MEMBRANES MEASURED BY FLUORESCENCE RECOVERY AFTER PHOTOBLEACHING (FRAP). J. Hochman, M. Schindler, J. Lee, J. Matia, S. Ferguson-Miller. Biochemistry Department, Michigan State University, East Lansing, MI 48824.

The mobility of tetramethyl rhodamine labeled cytochrome c was measured on membranes of giant mitochondria produced by feeding mice a diet containing cuprazone. The derivatized cytochrome c was extensively purified and found free of non-covalently bound dye. The derivative demonstrated electron transport activity in mitochondrial membranes. Cytochrome c-depleted giant mitochondria were swollen at 50 mM osmolarity to produce a smooth spherical form. Fluorescent cytochrome c was added at 20 μM and excess was removed by centrifugation and resuspension in 40 mM sucrose and 10 mM Hepes pH 7.2. Under these conditions, oxygen consumption was observed on addition of succinate. FRAP measurements on these mitochondria showed monophasic exponential recovery yielding a diffusion coefficient for cytochrome c of 1.7×10^{-10} cm^2/sec. This value is similar to that obtained for diffusion of cytochrome oxidase in inner mitochondrial membranes (Sowers and Hackenbrock, 1980, 38th Ann. Proc. Electron Microscopy Soc. Amer.). The results suggest that at least one cytochrome c is moving in association with the large integral membrane protein complex. This work was supported by NIH Grant GM 26916 (SFM).

W-AM-Po134 ESR LINESHAPES AND COOPERATIVITY IN THE MITOCHONDRIAL B CYTOCHROMES. J.C. Salerno, S.E. Kelly and T. Ohnishi*, Rensselaer Polytechnic Institute; *University of Pennsylvania.

Mitochondrial b cytochromes exhibit interesting anomolous properties, including low energy and pH dependent midpoint potentials and unusual ESR spectra with high apparent anisotropy. Cyt. b_{566} has an unusual assymmetric feature near g=3.75; cyt. b_{563} (in complex II) and cyt. b_{561} have more symmetric features near g=3.55 and 3.44. These signals are essentially pH independent between pH 6 and 10. Rapid passage experiments suggest $2.0>g_2>1.0$, $g_3<1.0$ for each.

The low field features can be simulated by assuming that the low temperature linewidths are due to a distribution of crystal field splittings. Variations in the rhombic splitting R dominate if variation of the tetragonal splitting V (along the heme normal) is not $>>\Delta R$. If the orbital reduction factor $K \sim 1.00$, V must be $\sim 3.3\lambda$ and R between 0 and $.5\lambda$ for b_{561}; R is larger for b_{563} and b_{561}. Reasonable spin quantization values require $1.04 \gtrsim K \gtrsim .99$, $3.8\lambda \geq V \geq 2.4\lambda$. Concentrations cannot be determined directly from present ESR spectra. The tetragonal splittings thus may be similar to that of cytochrome b_5. It is possible that all these cytochromes are bishistidine cases which differ in the relative orientations of the imidazole rings, although this is far from certain; other ligation schemes are consistent with the data.

In potentiometric titrations of ESR and/or optical spectra of bc_1 complex electron carriers, minor components (eg. a small fraction of cyt. b_{566} titrating with cyt. b_{561}) are at most a few percent of the total. Cooperative interactions between b_{566}, b_{561}, and Qc, and between b_{561}, cyt. c_1 and Reiske's Fe/S center, are therefore relatively small.

W-AM-Po135 LOW POTENTIAL EPR SIGNALS OF CYTOCHROME OXIDASE, G. Goodman (intro. by R. LoBrutto), Dept. of Biochem. and Biophys., Univ. of Penna., Phila., PA. The redox titration behavior of the low-spin and high-spin heme EPR signals has been studied as a function of pH. An attempt has been made to correlate the heme EPR signals with the low potential ($E_m \leq 240$ mV) optical absorbance transition at 605 nm (1). At pH 6.0, no low-spin heme EPR component appears with $E_m \leq 240$ mV. The axial and rhombic high-spin components are well developed at low potentials, and when maximally formed they represent approx. 100% of one heme, in general agreement with Lanne et al (2). The axial high-spin signal is the major component, corresponding to 60-75% of one heme. At pH 7.2, an EPR signal with g=3.03 appears at low potentials, with magnitude up to 40% of the fully oxidized g=3 signal. As the potential is increased more than half of this signal disappears, and a signal at g=3.06 is formed. The high-spin signals formed at low potential contribute maximally 35% of one heme. The axial signal represents <12% of one heme whereas the rhombic signal is the major component. Thus, the maximal magnitude of the rhombic signal is unchanged from the pH 6.0 case.

The results suggest that the axial high-spin heme signal and the g=3.03 signal are pH variants of the same species: a(ox)a_3(red). The rhombic signal corresponds to a(red)a_3(ox). This result supports the Wickström-Nicholls hypothesis (3): the low-potential optical 605 nm transition corresponds to oxidation of the fully reduced cytochrome aa_3 pair to an equilibrium mixture of a(ox)a_3(red) and a(red)a_3(ox).

Refs.: 1. Leigh, JS Jr., DF Wilson, CS Owen, and TE King, Arch Biochem and Biophys. 160, 476(1974). 2. Lanne, B, BG Malmström and T Vänngård, Biochim Biophys acta, 545, 205-214(1979). 3. Wickström, MKF HJ Harmon, WJ Ingledew and B Chance, FEBS Lett. 65, 259-277(1976).

W-AM-Po136 TWO PATHWAYS OF CYTOCHROME b REDUCTION IN UBIQUINOL-CYTOCHROME c OXIDOREDUCTASE OF MITOCHONDRIA AND PHOTOSYNTHETIC BACTERIA. K. Matsuura and P.L. Dutton, U. of Penn., Phila., PA 19104

Using a hybrid system of mitochondrial ubiquinol-cytochrome c oxidoreductase and reaction center of Rps. sphaeroides (1,2), we have studied pathways of flash induced cyt. b reduction. When Q_7H_2 is present, a flash elicits simultaneous reduction of cyt. b_{562} (and/or b_{566}) and of photooxidized cyt. c + c_1. The presence of cyt. c as well as antimycin was necessary to observe these reactions. When oxidized Q_7 is present, a flash elicits a cyt. b_{562} reduction without simultaneous reduction of cyt. c + c_1. Furthermore, cyt. b_{562} reduction was observed in a system even lacking cyt. c with Rieske FeS and cyt. c_1 reduced before and during the b reduction. Two pathways of cyt. b reduction are apparent from these results; one is "oxidant induced reduction" and the other is "direct one electron reduction" from the reducing side. These pathways are integrated into the proposal of Figure 1 which now includes: 1. Reaction center components (e.g. Q_B) which reduce Q_7 to Q_7^- possibly through a close association with the oxidoreductase, or reduce Q_7 to Q_7H_2 probably through the pool quinone. 2. High redox potential components in the form of a linear electron transfer sequence, FeS→c_1→c, which oxidize Q_7H_2 to Q_7^-. 3. A Q_7 pocket which has at least three different functioning sites symbolized in Figure 1 as a triangle and indicating three redox species of Q_7 which are dominant at each site. 4. Cyt. b which can be reduced or oxidized by Q_7^- formed either by the reducing route or the oxidizing route. 5. These elements are equipped to generate the prerequisite redox state, ferrocyt. b-Q_7^-, for the electrogenic reaction (3). 1.PNAS 77 6339 1980 2.FEBS Lett. 131 17 1981 3.Biophys. J. 33 102a 1981 Supported by NIH GM 27309

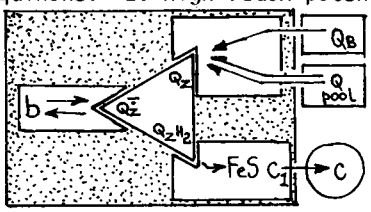

W-AM-Po137 THE NATURE OF "INVISIBLE" COPPER IN CYTOCHROME OXIDASE. Kamal de Fonseka and Britton Chance, Johnson Research Foundation, University of Pennsylvania, School of Medicine, Philadelphia, PA 19104

Data obtained by X-ray absorption spectroscopy (edge and EXAFS studies) as well as by determinations of the amino acid sequence of subunit II have indicated the type I "blue" copper nature of Cu_{a3}. Complementary data on the contribution of Cu_{a3}^{2+} to the 700-900 nm band of the resting enzyme are obtained by disequilibration of the copper components [Cu_a^+ Cu_{a3}^{2+}], by reduction (5 mM ascorbate, 20°C) of cytochrome c depleted mitochondria in the presence of 1M formate, and freeze-trapping the samples after appropriate reduction times. The near i.r. band shapes vary considerably with the progress of the reaction. Comparison with the fully oxidized and reduced samples enables us to delineate a band at 765 nm (width at half-height = 60 nm, $\varepsilon_{max} \geq 1\ mM^{-1}\ cm^{-1}$) which we attribute to Cu_{a3}^{2+}. The maximum disequilibration gives [90% Cu_{a3}^{2+}, 61% Cu_a^{2+}]. This band is much broader and 5 to 10 times more intense than the heme (d-d) bands in this region. The band position depends on the redox state and liganding of the redox centers. Thus, in the initial stages of reoxidation of fully-reduced or mixed valence cytochrome oxidase, i.e., in Compounds B_1 and C, the band maximum occurs at 780 nm and 748 nm, respectively. The crucial catalytic role of Cu_{a3} is also demonstrated by these observations. Rapid redox equilibration between Cu_a and Cu_{a3} could make the 700-900 nm band behave homogeneously (1,2) and may lead to erroneous conclusions as to its origin, unless precautions are observed to achieve disequilibration. (Supported by NIH Grants GM 27308 and HL 15061 and by SSRL Project 423B (NSF,DDR,DOE).

1. Beinert et al (1980) Biochim.Biophys.Acta 591:458-470
2. Boelens & Wever (1980) FEBS. Lett.116:223-226.

W-AM-Po138 COUPLING OF STRUCTURAL CHANGES AND CHARGE SEPARATION IN CYTOCHROME OXIDASE.B.Chance, Johnson Research Fnd.,U. of PA,Phila,PA. and L.Powers,Bell Labs,Murray Hill,NJ.

The probable location of the redox center of cytochrome oxidase on the cytosolic side of the membrane(1)from the Cu edge(2)and sequence studies (R.Capaldi,pers.commun)plus the high H+/e⁻ values observed(3)appear to require a proton pump(4)and make transmembrane electron transfer unneccessary (5). Conservation of energy from chemical bond making and breaking, for example the peroxide and S bridges between the metal atoms of the redox center and the motion of the Fe and Cu atoms with respect to each other (6)may be directly linked to hydrogen ion transport via the S atom operating within a transmembrane channel formed by subunits II or III(Capaldi,pers.commun.), or indirectly linked to nearby carboxyl groups via linked functions as in the Bohr effect for hemoglobin(1,7).(1)B.Chance, "Relationship between Structure and Function in Biochemical Systems" Symposium,Rome,1981.(2)L.Powers et al,BBA546:520-538,1979.(3)A.Lehninger et al, in Mitochondria and Microsomes(Lee et al,eds)Addison-Wesley Reading,MA459-479,1981.(4)K.Krab and M.Wikstrom,BBA504:200-214,1978. (5)P.Mitchell, Chemiosmotic Coupling and Photosythentic Phosphorylation,Glynn Res.,Bodmin,Cornwall.(6)L.Powers et al, Biophys.Jour 34: 465-498,1981.(7)B.Chance, in Mitochondria and Microsomes(op.cit.)271-292. Supported by NIH grants GM27476,28385,27303;HL-SCOR-15061:SSRL Project 423B(NSF,DDR,DOE).

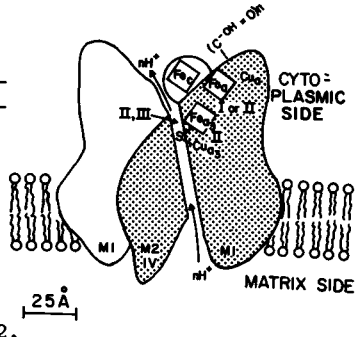

W-AM-Po139 CYTOCHROME OXIDASE: STRUCTURE AND MECHANISMS, REDOX STATES, OXYGEN INTERMEDIATES, PULSED AND CU-DEPLETED FORMS - A SYNCHROTRON X-RAY STUDY. L.Powers, Y.Ching, Bell Labs, Murray Hill, NJ; B.Chance, Johnson Research Foundation, U.of PA, Phila, PA; B.Muhoberac, U.of Texas, San Antonio, Texas.

The structure of the redox sites of cytochrome oxidase reported in this journal(1,2)has been supported further in studies in collaboration with Wharton et al(3)on the Cu-depleted oxidase. There is neither a S-bridge nor a third shell backscattering atom due to Cu in the iron EXAFS of the active site confirming and extending the structure previously presented(1,2). The Fe has a S ligand at 35% occupancy at 2.28Å in agreement with EPR data(3). The pulsed oxidase(4)is a modified form whose EPR and optical properties have remained enigmatic. EXAFS show that the S atom no longer bridges the Fe and Cu but is bound to Cu as a cysteinyl residue. Doubt is cast on the functional role of the pulsed oxidase structure in the redox cycle since Cu edge spectra, which clearly distinguish the pulsed oxidase, show the end product formed sequentially from oxy- and peroxycytochrome oxidase intermediates exhibits the Cu edge structure characteristic of the S-bridged form. Mechanisms involving cyclic formation of oxy-, peroxy-, and S-bridged compounds are supported(1).

(1).Powers et al, Biophys.Jour.33:2(2)94a,1981(2)B.Chance and L.Powers, Biophys.Jour33:2(2)94a,1981. (3)S.Weintraub and D.Wharton, J.Biol.Chem.254(4)1669-1676,1981.(4)E.Antonini et al., Proc.Natl.Acad. Sci.(USA)74(8)3128-3132,1977.

Supported by NIH GM27308,27476,28385,HL-SCOR-15061,SSRL Project 423B(DDR,DOE,NSF).

W-AM-Po140 ^{1}H NMR STUDIES OF UBIQUINONE-LIPID INTERACTIONS IN DMPC VESICLES. Eldon L. Ulrich, Mark E. Girvin, John L. Markley, and William A. Cramer, Departments of Chemistry and Biological Sciences, Purdue University, West Lafayette, Indiana 47907.

Using ^{1}H NMR spectroscopy at 470 MHz, we have investigated interactions of ubiquinones (UQ) with dimyristoylphosphatidylcholine (DMPC) in sonicated vesicles. The lipid phase transition in the vesicles can be determined from the temperature dependence of the chemical shift of the interior choline methyl proton peak. Phase transition temperatures are observed for DMPC vesicles and vesicles containing 5 mole % UQ_{10} or UQ_2 at 22, 17, and 18 ± 1 °C, respectively. UQ_2 does not affect the cooperativity of the transition, but UQ_{10} greatly broadens the transition. UQ_{10} proton peaks can still be observed at 7 °C where the lipid resonances have broadened out, indicating that at low temperatures the UQ is more mobile than the DMPC and may form a pool within the membrane.

The DMPC tail methyl proton resonance is split into two peaks which have an intensity ratio of 1.8:1 with the more intense peak being at high field. As the concentration of UQ_{10} or UQ_2 is increased from 0.5 to 10.0 mole %, the higher-field peak decreases in intensity, and an increase in intensity is observed at lower field. With UQ_{10}, approximately 20% of the lipid tail methyl groups are affected. This effect saturates at about 2 mole % UQ_n, which is near the physiological concentration of UQ_n in biological membranes. The presence of UQ_n in sonicated DMPC vesicles changes the environments of the lipid head group, chain acyl, and tail methyl protons in a manner depending on the length (n) of the UQ isoprenoid chain. This work was supported by grants from the USDA (#5901141080l600), NIH (#RR 01077), and NSF (#PCM-8022807).

W-AM-Po141 TUNNELING IN BIOMOLECULES:ELECTRONS AND MOLECULES - A. Chang, R. Austin and P. Watnick (Princeton University)

We have used optical excitation and high magnetic fields in a broad-ranging study of tunneling processes in biomolecules. The two systems studied are electron transfer in cytochrome c and carbon-monoxide tunneling in heme proteins. The cytochrome c work uses photo-induced charged transfer and T-jump to study the return to equilibrium of an electron transferred between two redox sites. The high magnetic field is used to probe the recombination of carbon monoxide with myoglobin and hemoglobin at low temperatures. The magnetic field affects both the quantum yield of photolysis and the recombination rate. A theory has been developed to explain these results.

W-AM-Po142 PROBING THE MECHANISM OF RAT LIVER F_1-ATPase WITH THE PHOTOAFFINITY LABEL BENZOYL BENZOYL ATP. P.S. Coleman and N. Williams, Lab. of Biochemistry, Dept. of Biology, New York University, New York, N.Y. 10003.

Rat liver mitochondrial F_1, an oligomeric enzyme (with probable subunit stoichiometry: $\alpha_3\beta_3\gamma\delta\varepsilon$) is the only mammalian F_1-ATPase so far examined via X-ray crystallography (Amzel, J. Bioenerg. Biomemb. 13, 109, 1981). We have synthesized and used a new photoaffinity analog of ATP, 3'(2')-O-(4-benzoyl)benzoyl ATP, (BATP), as a probe for the mechanism of rat liver F_1-catalyzed hydrolysis. BATP is a good substrate for F_1, yielding an apparent K_m identical to that with ATP and an apparent V_{max}= 12% that for ATP. The analog binds to F_1 covalently upon illumination ($\lambda > 340$ nm) at sites presumed specific for ATP and, subsequent to hydrolysis, for ADP. Data from F_1 BATP kinetics and radiolabelling PAGE patterns (with ^3H- and ^{32}P-BATP) allow formulation of a minimal catalytic mechanism of action for F_1. Our proposal is consistent with data of others, and is supported by the radiolabelled PAGE patterns of steady-state (i.e., non-equilibrium) BATP hydrolysis $\pm Mg^{2+}$, during light-induced covalent attachment of BATP to soluble F_1. The mechanism visualizes a catalytic cleft at an α/β subunit interface on F_1, with ATP hydrolysis effected at an ATP(Mg^{2+}) binding site on β, and a regulatory ADP binding site on the closely apposing α subunit. In a sequence of steps, ATP hydrolysis at β releases P_i to the medium while the resulting ADP is sequestered at the α site. A second molecule of ATP(Mg^{2+}) then binds to the now empty β site, inducing, via conformational adjustment, release of ADP at α. ADP, binding to a different site than ATP, is thus not a competitive inhibitor.

W-AM-Po143 PROTON PUMPING CAN NOT BE DEDUCED FROM PH CHANGES. by Peter A. Stewart, Physiology/Biophysics, Brown University, Providence, R.I., 02912.

The behavior of hydrogen ions in aqueous solutions is different from that of strong ions such as K^+, Na^+, or Cl^-; hydrogen ions participate in rapidly equilibrating reactions, most notably water dissociation, whereas strong ions are essentially non-reacting. As a result, hydrogen ion concentration (or activity), $[H^+]$, is a dependent variable, not an independent variable. The numerical value of $[H^+]$ at any instant is determined by the strong ion concentrations, and by the CO_2 partial pressure, PCO_2, if CO_2 is present. If PCO_2 is kept constant, then $[H^+]$ changes can be brought about by changing the strong ion concentrations, but not simply by transporting hydrogen ions into or out of the solution. This somewhat counter-intuitive statement can be derived from elementary chemical principles very easily ("How to Understand Acid-Base" by Peter A. Stewart, Elsevier N.Y. 1981). Details of the derivation will be presented. It requires us to recognize that pH changes measured in solutions containing suspended cells, mitochondria, chloroplasts, or other membrane-bound entities, can be interpreted as evidence for strong ion movements across the membranes, but not as evidence for H^+ movements ("proton pumping"). If the solutions in question also contain weak acids or bases ("buffers"), then the calculations become more complex, but the same conclusions obtain: pH changes do not mean that hydrogen ions have been moved into or out of a solution. Significant re-evaluation and re-interpretation of much of the current literature on mechanisms of ATP formation seems called for.

W-AM-Po144 TEMPERATURE EFFECTS ON OXIDATIVE PHOSPHORYLATION. B. D. Jensen and T. E. Gunter Dept. of Rad. Biol. and Biophysics, Univ. of Rochester, Rochester, N.Y. 14642

The mechanism of oxidative phosphorylation is not completely understood. To gain useful knowledge in this area the parameters of ΔpH, $\Delta\Psi$ and the rates of oxidation and phosphorylation need to be determined accurately and interrelated under steady-state conditions. Accuracy requires the use of high concentrations of mitochondria. The antagonistic requirement of maintaining a non-rate limiting oxygen concentration in the presence of large amounts of mitochondria make measurement at low temperature a necessity. Therefore, ΔpH, $\Delta\Psi$ and the rates of oxidation and phosphorylation were measured simultaneously and quantitatively over a broad range of carefully controlled temperatures. ΔpH was measured by the [C-14]-acetate distribution technique and by determining the intramitochondrial volume using [C-14]-sucrose exclusion. $\Delta\Psi$ was quantitated by examining the tetraphenylphosphonium cation distribution with an electrode built as described (Kamo, et. al.,1979). Oxygen was measured with a Clark type polarigraphic electrode and ATP was quantitated by [P-32]-phosphate incorporation followed by extraction of remaining phosphate as described (Rose and Ochoa, 1955). Preliminary studies indicate that the phosphorylation driving forces remain remarkably constant (ΔpH=0.5, $\Delta\Psi$=200mv) over a wide range of temperatures (8-25°C), while the rates of oxidation and phosphorylation decrease markedly at low temperature. This suggests that many enzyme systems, both directly and peripherally involved in oxidative phosphorylation change in concert over a broad temperature range while maintaining appropriate thermodynamic interrelationships. Supported by NIH (AM-20359) and DOE (DE-AC02-76EV03490).

W-AM-Po145 RATES OF Ca^{2+} EFFLUX AND H^+ INFLUX ACROSS THE INNER MITOCHONDRIAL MEMBRANE. T.E. Gunter, J.H. Chace, and K.K. Gunter. Dept. of Rad. Biol. and Biophys., Univ. of Rochester, NY.

Rat liver mitochondria were suspended at 2 mg/ml protein in 0.3 OsM 3:1 mannitol-sucrose, containing 0.1 mM $MgCl_2$, 0.5 mM Na succinate, 3 mM Na Ac and 5 μM tetraphenyl phosphonium. Ca^{2+} activity was measured using a Radiometer F2002 electrode, pH using a Markson S785 electrode, and the membrane potential using a homemade tetraphenyl phosphonium electrode. Internal water volume was measured as previously reported. Calibration of the buffering power of the medium containing ruthenium red inhibited mitochondria, for both Ca^{2+} and H^+, allowed direct conversion of the readout into amount of ion permeating the membrane. In a series of experiments, 60 to 100 nmoles Ca^{2+}/mg protein was added to the suspension, followed 4 minutes later by 4 nmoles ruthenium red/mg protein and 3.3 μg/ml oligomycin. Efflux of Ca^{2+}, influx of H^+ and membrane potential were monitored following the above additions, over a range of pH from 6.3 to 9.0, both with and without selected additions of ATP, cyanide, antimycin A, CCCP, oxaloacetate, and acetoacetate. The following generalizations could be made about the results. There is a consistent decrease in the rate of H^+ influx and a small, inconsistent decrease in the rate of Ca^{2+} efflux with increasing pH. Membrane potential breakdown has a varying effect on increasing the rate of Ca^{2+} efflux, sometimes doubling the rate and sometimes having no effect. Oxaloacetate or acetoacetate usually increase both the rate of Ca^{2+} efflux and the rate of H^+ influx and sometimes decrease the membrane potential. Below a pH of 6.8, with anti A inhibited mitochondria, it is possible to obtain data in which the rate of Ca^{2+} efflux approximately equals one half of the rate of H^+ influx. At higher pH the rate of Ca^{2+} efflux is often much higher than the rate of H^+ influx under both active and passive conditions. Supported by NIH (AM-20359) and DOE (DE-AC02-76EV03490).

W-AM-Po146 INHIBITION OF THE MITOCHONDRIAL K/H EXCHANGER BY H^+ AND MG^{2+} IONS. William H. Martin* and Keith D. Garlid, Dept. of Pharmacology, Medical College of Ohio, Toledo, Ohio 43699

Several techniques for studying the mitochondrial K/H exchanger have been developed (Garlid, K. D., J. Biol. Chem. 255, 11273-11279, 1980) which permit further characterization of its properties and kinetics. In the present study we monitored K+ movement with an ion electrode, and matrix volume by absorbance at 520 nm in suspensions of rat liver mitochondria oxidizing succinate at 25°C. Variations in matrix Mg^{2+} were achieved by matrix swelling, by the addition of citrate, or by the addition of A23187. In each case efflux was identified as K/H exchange by the fact that it was reversed by valinomycin.

In accord with the Mg^{2+} carrier brake hypothesis, we observed increased rates of K+ efflux with decreased levels of free Mg^{2+}. In the absence of Mg^{2+} the Vmax was estimated to be 300 nmol K+/min·mg protein. H+ ions were found to inhibit K/H exchange over the range studied, pH 6.7 to 8.0. Plots of inverse velocity against $[H+]^2$ were linear, indicating that H+ ions inhibit at a separate site in addition to the transport site. While K/H exchange increases with increasing pH, Na/H exchange exhibits a peak at pH 7.0 to 7.2. This difference in pH profiles may reflect operation of separate antiporters for Na+ and K+. On the other hand, a single cation antiporter may exhibit these characteristics if Na+ can interact with the proton inhibitory site. If the latter explanation is correct, it implies that decreased rates of Na/H exchange at alkaline pH are due to auto-inhibition by Na+. (Supported by USPHS grant GM 24297)

W-AM-Po147 UNIDIRECTIONAL PHOSPHATE TRANSPORT CATALYZED BY THE PURIFIED MITOCHONDRIAL PHOSPHATE TRANSPORT PROTEIN. Hartmut Wohlrab and Nancy Flowers. Boston Biomedical Research Institute, 20 Staniford Street, Boston, MA 02114, and Department of Biological Chemistry, Harvard Medical School.

The mitochondrial phosphate transport protein has been copurified from beef heart mitochondria with the adenine nucleotide translocase (Wohlrab, H. (1980) J. Biol. Chem. 255, 8170-8173). We have now incorporated this protein into liposomes prepared from purified soybean phosphatidylethanolamine, soybean phosphatidylcholine, and egg phosphatidic acid and determined phosphate:phosphate exchange rates and unidirectional phosphate flux rates. With the intraliposomal pH (pH_i) the same as the extraliposomal pH (pH_e), we found a K_m for phosphate:phosphate exchange of 2.5 mM. This K_m appears to be independent of the intraliposomal phosphate concentration $[(P_i)_i]$. The V_{max} at an extrapolated infinite $[(P_i)_i]$ is 12 mol/min mg protein. Unidirectional phosphate transport was determined with initial $[(P_i)_e] = 1.0$ mM and $[(P_i)_i] = 0.0$ mM. The phosphate uptake is essentially complete at 30 s and we determined the amount of phosphate taken up as a function of initial pH_e and pH_i. With $pH_e = pH_i = 6.8$, 0.13 mol/mg protein are taken up and at $pH_e = 6.8$, $pH_i = 8.0$, 0.45 mol/mg protein are taken up. This experiment demonstrates that pH gradient, alkaline inside, increases the amount of phosphate taken up. The initial rate of the unidirectional phosphate flux ($pH_i = 8.0$, $pH_e = 6.8$, $[(P_i)_i] = 0.0$ mM, $[(P_i)_e] = 1.0$ mM) is 2 mol/min mg protein or 8 mol/min mg phosphate transport protein without the adenine nucleotide translocase. Supported by NIH and NSF.

W-AM-Po148 RUTHENIUM RED (RR) INDUCTION AND ROTENONE REVERSAL OF UNCOUPLER-STIMULATED K^+ RELEASE FROM BEEF HEART MITOCHONDRIA. D.W. Jung and G.P. Brierley, Department of Physiological Chemistry, Ohio State University, Columbus, Ohio 43210

We have previously reported (JBC, in press) that uncoupler (CCP) induced efflux of K^+ from heart mitochondria occurs when (1) CCP is present initially with low concentrations of calcium chelator or (2) CCP is added after one min of respiration-dependent Pi uptake. RR will substitute for chelator in reaction (1) with 1 μM increasing efflux of ^{42}K from labeled mitochondria from a control level of 17% to 87% at 3 min. The RR dose response curve for $^{42}K^+$ efflux is almost identical to that for the inhibition of Ca^{++} uptake. RR + CCP-induced K^+ efflux is completely blocked by rotenone and unlike reaction (1) is not inhibited by added Ca^{++}. Neither RR nor CCP induces K^+ release alone. Reaction (2) is also blocked by rotenone and when rotenone is added after CCP the release of K^+ is halted regardless of whether or not respiration continues. The pyridine nucleotide (PN) pool is almost completely oxidized following CCP addition, but subsequent addition of rotenone results in considerable PN reduction. These findings parallel observations made on Ca^{++} uptake and release and suggest that CCP-induced K^+ release occurs via the Ca^{++} uniporter. Further, it appears possible that alterations on both the cytosol side (removal of Ca^{++} by chelator or uptake into the matrix, or alteration of carrier by RR) and matrix side (oxidation of PN) may be required for K^+ efflux. ADP also decreases K^+ permeability and appears to be a regulatory factor. The closing of this uncoupler-dependent K^+ pathway by rotenone also suggests a regulatory role for pyridine nucleotides in controlling activity of the Ca^{++} channel under conditions where nonspecific permeability changes are not induced. (USPHS Grant HL09364.)

W-AM-Po149 IN VIVO ^{31}P and ^{13}C NMR MEASUREMENTS OF THE EFFECTS OF SATURATED FATTY ACIDS ON BACTERIA: UNCOUPLING, SPECIFIC METABOLIC INHIBITIONS, AND STEADY-STATE KINETICS OF UPTAKE. R. V. Mustacich, D. S. Lucas, and F. S. Ezra. The Procter & Gamble Co., Cincinnati, Ohio.

In vivo ^{31}P NMR measurements have been used to determine the concentration dependence of chemiosmotic uncoupling in bacteria by saturated fatty acids. *E. coli* is shown to have a transmembrane pH gradient (ΔpH) which is much less stable and decays with time relative to *S. aureus*. Following this decay, the ΔpH of *E. coli* is collapsed more slowly than that of *S. aureus* as a function of fatty acid concentration. The cytoplasmic orthophosphate resonance of *S. aureus* is also observed to broaden with anaerobiosis and narrow with oxygenation of the cell suspension. ^{13}C NMR of bacterial fermentation of ^{13}C enriched glucose together with glucose assay suggests the phosphoenolpyruvate:phosphotransferase as the site of inhibition by octanoic acid. The inhibition of lactate transport by octanoic acid is also observed by ^{13}C NMR. In combination with ^{14}C octanoate distribution measurements, the ^{31}P NMR data provides estimates of the ratio of the permeability coefficients of the free fatty acid to the acid anion for the bacterial membranes. The steady-state application of the Goldman-Hodgkin-Katz equation to the ΔpH collapse data is derived with a discussion of the chain length dependence of the steady-state kinetics of uncoupling by the saturated fatty acids.

W-AM-Po150 RATE LIMITATION OF STATE 3 OXIDATIVE PHOSPHORYLATION BY ADP/ATP TRANSLOCATION. John J. Lemasters, Ron Grunwald and William H. Billica, Laboratories for Cell Biology, Department of Anatomy, University of North Carolina, Chapel Hill, NC 27514.

Inhibition of state 3 oxidative phosphorylation by rotenone, antimycin, oligomycin and atractyloside was examined in rat mitochondria. To assure equilibration with their binding sites, the inhibitors were preincubated with mitochondria for 14 minutes before measuring ADP stimulated oxygen uptake. Using either succinate or glutamate plus malate as respiratory substrate, inhibition curves for atractyloside were hyperbolic while inhibition curves for oligomycin, antimycin and rotenone were sigmoidal. Hill plots gave slopes close to 1 for atractyloside inhibition and 3.4, 4.6 and 2.6, respectively, for oligomycin, antimycin and rotenone inhibition, where a slope of 1 signified hyperbolic inhibition and slopes greater than 1 indicated sigmoidal inhibition. Atractyloside inhibition remained hyperbolic between pH 6.5 and 7.7, between 9° and 37°C, and with other respiratory substrates such as 3-hydroxybutyrate and pyruvate plus malate. The data indicate that state 3 respiration is proportional to the number of catalytically active adenine nucleotide carriers. It is concluded that the atractyloside sensitive ADP/ATP translocation reaction is rate-limiting in mitochondrial oxidative phosphorylation and that the antimycin, rotenone and oligomycin sensitive reactions of respiration and ATP synthesis are not. Supported by GM 28999 and 79-1013.

W-AM-Po151 EVIDENCE AGAINST ABSOLUTE CONTROL OF RESPIRATION BY EXTRAMITOCHONDRIAL PHOSPHORYLATION POTENTIALS OR BY [ATP]/[ADP] RATIOS. W.E. Jacobus, R.W. Moreadith, K.M. Vandegaer*, Medicine and Physiological Chemistry, The Johns Hopkins University School of Medicine, Baltimore, MD 21205.

To explore how mitochondria respire at high, physiological phosphorylation potentials, intact rat liver mitochondria were incubated in oxygraph medium containing 5 mM succinate, 1.0 mM ATP and 20 mM glucose, pH 7.2 at 37°C. Yeast hexokinase (0.02 to 1.0 IU) was added to establish steady-state rates of respiration. Samples were removed, assayed for ATP, ADP, and Pi content, and ratios were calculated. As previously reported, low rates of respiration were observed at high phosphorylation potential ([ATP]/[ADP]x[Pi]) or [ATP]/[ADP] ratios, and rates of respiration increased as these values declined. In a second series, hexokinase was held constant at 0.35 IU, an amount which stimulated respiration to 90% ADP State 3. ATP (5 μM to 10 mM) was titrated to establish steady-state rates of oxygen consumption. Under these conditions, low rates of respiration correlated with low [ATP]/[ADP] ratios and extramitochondrial phosphorylation potentials, while maximum rates of respiration were observed at high values. Therefore, it may be concluded that these extramitochondrial parameters per se exert little or no regulatory influence on the rates of respiration, or matrix ATP synthesis. In both cases the concentrations of ADP correlated to respiratory rates. Double-reciprocal plots were used to estimate the apparent K_m ADP for respiratory stimulation. The values are 56 μM for constant [ATP] and 15 μM at constant hexokinase. The value calculated from direct ADP pulses was 25 μM. Together, these results suggest that respiration is controlled by the availability of ADP and the kinetics of its transport by the adenine nucleotide translocase, a hypothesis proposed by Chance and Williams 25 years ago.

W-AM-Po152 INTRACELLULAR pH CHANGES DURING TRANSITIONS BETWEEN ANAEROBIC DORMANCY AND AEROBIC DEVELOPMENT IN ARTEMIA EMBRYOS. Wm. B. Busa[1], J.H. Crowe[1] and G.B. Matson[2], Depts. of [1]Zoology and [2]Chemistry, University of California, Davis, CA 95616.

When deprived of O_2, encysted gastrula-stage embryos of the brine shrimp Artemia enter metabolic and developmental dormancy and survive in this state at least 5 months, during which time no detectable carbohydrate metabolism occurs (for review see Clegg and Conte in: The Brine Shrimp Artemia, Vol. 2 pp 11-54, Persoone, G. et al eds. Universa P., Wetteren, Belgium, 1980). Using ^{31}P NMR we have achieved the first observations of the internal ionic environment in these embryos, which resist microelectrode and radiolabel methodologies due to their semi-permeable shells. pH_i of anaerobic dormant cysts (=6.3 to 6.7, determined by P_i chemical shift) is independent of buffer pH (pH_o) over at least pH_o 4 to 8. When aerobiosis is initiated via O_2-saturated superfusion pH_i increases, exceeding the useful range of P_i as an indicator (aerobic $pH_i \geq 7.9$). The reverse transition, from aerobic development to anaerobic dormancy, displays a >1.5 ppm P_i chemical shift decrease reflecting a >1 unit pH_i decrease, which cannot be attributed to lactate accumulation (Ewing and Clegg, 1969. Comp. Biochem. Physiol. 31, 297-307).

The low pH_i of anaerobic dormant embryos suggests an explanation for the unusual pH-activity profile of the cyst nucleoside enzyme P^1,P^4-diguanosine-5'-tetraphosphate synthetase (GP_4G synthetase), which is maximal at pH 6 and inactive at pH 8 (Warner et al, 1974. Can. J. Biochem. 52, 231-240). Thus, the low dormant pH_i is consistent with the notion (see Clegg and Conte, p.c.) that catabolism of the cyst's large GP_4G stores may meet the embryo's minimal energetic requirements during anaerobic dormancy. NSF grant PCM 80-04720 and National Sea Grant RA/41.

W-AM-Po153 ^{31}P-NMR STUDIES OF BARNACLE MUSCLE BUNDLES AND SINGLE CELLS. G.R. Dubyak, A. Scarpa, J. Engle, and M. Cohn. Dept. Biochem-Biophys., Univ. Pennsylvania, Philadelphia, PA 19104 USA.

P-NMR spectra (145.7 MHz) were obtained from barnacle muscle bundles and single muscle cells. Samples containing muscle bundles (500 mg wet wt.), immersed in Ca^{++}-free saline, were scanned using 90° pulses with delay times ranging from 1 to 10 sec; 100 scans were sufficient to obtain spectra with excellent S/N. Spectra obtained within 30 min after dissection reveal a major peak at 3.5 ppm (relative to external phosphoric acid) corresponding to phosphoarginine (PA), and three smaller peaks arising from the γ (4.9 ppm), α (9.9 ppm), and β (19 ppm) moieties of ATP. Initially, no resonances are observed at -5 or -2.6 ppm, indicating that little (< 100 μM) sugar phosphate (SP) or inorganic phosphate (Pi) is present in this muscle under resting conditions. As the post-dissection incubation time is prolonged, PA gradually decreases with concomitant increases in SP and Pi, bu but no change in ATP. The rates of SP and Pi accumulation are not affected by the presence of cyanide. Conversely, SP, but not Pi, accumulation is accelerated in the presence of iodoacetamide. The observed chemical shift of Pi and the separation between the α and β peaks of ATP are consistent with the intracellular pH of 7.3 and pMg of 2.2 which characterize these cells. Identical results were obtained with a single muscle cell (15 mg wet wt.) mounted in a 2 mm (O.D.) capillary tube, which, in turn, was held in a horizontal 2.2 mm (I.D.) solenoid receiver coil. With this apparatus, spectra with adequate S/N could be obtained in 20 min. In addition to providing a single cell system for NMR studies, the large size of these cells permits intracellular injections of normally impermeable compounds and kinetic analysis of their effects on cellular metabolism. (This work was supported by NIH grant HL-15835 and an MDA fellowship to G.R.D.)

W-AM-Po154 Na-K-ATPase is not inefficient in the Rous sarcoma transformed HTC-BH cell. R.S. BALABAN and J.P. BADER*, National Heart, Lung, and Blood Institute, Laboratory of Kidney and Electrolyte Metabolism, and *National Cancer Institute, NIH, Bethesda, MD 20205

Recently it has been proposed based on studies with isolated enzyme preparations that a characteristic of cellular transformation is a phosphorylation of the Na-K-ATPase ion pump which results in the pump operating inefficiently. To test this hypothesis in the intact cell, we determined the ratio of ouabain sensitive K uptake to oxygen consumption (QO_2) in intact RSV-HTC-BH cells. The instantaneous K uptake was determined during the reintroduction of K to K-depleted cells using an extracellular K-sensitive electrode. Simultaneously, QO_2 was determined with an oxygen sensitive electrode. To simplify the analysis, glucose was omitted from the media and replaced with lactate which eliminated aerobic glycolysis as a source of ATP. The results are given in the following table: *(Nmoles/min/mg protein)

K uptake rate*	ΔQO_2*	K/O_2	K/ATP	N
45.3 ± 1.5	3.68 ± 0.3	12.8 ± 1.0	2.14 ± 0.3	9

The K/ATP ratio was calculated using a stoichiometry of 6 ATP/O_2 for aerobic respiration. Ouabain (5×10^{-4} M) inhibited both K uptake and the stimulation of QO_2 by the reintroduction of K. Anoxia, in the absence of glucose, inhibited K uptake. These data suggest that Na-K-ATPase is operating at the normal stoichiometry of 2K/ATP in these transformed cells. Therefore, in these intact transformed cells the efficiency of Na-K-ATPase is the same as previously measured in non-transformed cells.

W-AM-Po155 THE REGULATION OF GLYCOLYSIS IN THE LENS. John K. Wolfe, Benigno D. Peczon, and Leo T. Chylack, Jr., Eye Research Institute and Howe Laboratory of Ophthalmology, Harvard Medical School, Boston, MA 02114

Rates of lens glycolysis have been determined by measuring the incorporation of ^{14}C into glycolytic intermediates starting with ^{14}C-labeled glucose in lens homogenates. Samples taken from the incubation mixture at various times were de-proteinized and applied to an anion exchange column which separated glycolytic intermediates. ^{14}C in fractions was determined by liquid scintillation counting. Results are expressed as per cent distriubtion of the ^{14}C among the glycolytic intermediates. A model was developed to describe the rate of glycolysis and the incorporation of ^{14}C into intermediates, using equations for the hexokinase (HK), glucose-6-phosphate dehydrogenase (G6PDH), and phosphofructokinase (PFK) reactions. Calculated HK activity includes inhibition by G6P, and calculated PFK activity includes inhibition by ATP and activation by cAMP. Results show that calculated distribution of the ^{14}C agrees very well with the experimentally determined distribution. We conclude that the equations for HK, G6PDH, and PFK can be used to describe the activity of the glycolytic system in the lens.

W-AM-Po156 MAGNESIUM-INDUCED APPARENT UNCOUPLING OF CALCIUM TRANSPORT AND SR ATPase ACTIVITY : THE ROLE OF THE CALCIUM-PRECIPITATING OXALATE.
Philippe Champeil, Daniel Gillet and Florent Guillain . Département de Biologie C.E.N. Saclay, F-91191 Gif-sur-Yvette Cedex, France.

We measured in parallel the ATPase activity and the calcium accumulation velocity of Sarcoplasmic Reticulum vesicles incubated with various amounts of magnesium (100 mM KCl, 20 mM Mops, pH 7, 20°C, 0.1 or 1 mM ATP, 0.1 mM Ca, 5 mM oxalate). High magnesium concentrations inhibited ATPase activity but also reduced to very low values the steady state coupling ratio of ATP hydrolysis to calcium transport. This apparent uncoupling was in fact likely to be due to the lowering of the free concentration of the calcium-precipitating oxalate as a result of the complexation of magnesium to oxalate. Related considerations might explain some published reports in which various treatments were found to affect the tight coupling of the SR calcium pump.

W-AM-Po157 NMR STUDIES OF CATARACTOGENESIS IN RABBIT AND HUMAN LENSES. J. Willis, R.G. González, P. Campbell, C. Serdahl, J. Newman, G.B. Matson*, L.T. Chylack, Jr.** and T. Schleich, Department of Chemistry, University of California, Santa Cruz, *University of California, Davis, NMR Facility, and the **Howe Laboratory of Ophthalmology, Harvard Medical School, Boston, MA.

We are currently studying the sorbitol and glycolytic pathways as well as related bioenergetic processes in single, intact, viable, rabbit and human lenses by C-13 and P-31 NMR spectroscopy, thereby providing a new non-invasive methodology for the study of sugar cataractogenesis, a complication of diabetes. A typical experiment consists of incubating a lens in an NMR tube fitted with a Teflon stage containing TC-199 medium (balanced to 290 mOsm/L) with supplemental C-13 C(1)-enriched glucose to either simulate normal (5.5 mM) or highly elevated (35.5 mM) conditions. The results to date are: (i) in rabbit lenses sorbitol production as a function of time under a high glucose stress is consistent with previous studies using an invasive methodology; (ii) limited studies with normal human lenses suggest that enhanced sorbitol production under a glucose stress occurs during the second 24 hr incubation period, rather than the first, implying the occurence of a lag period; (iii) cataractous human lenses (obtained by intracapsular extraction) appear not to be highly metabolically active in either sorbitol or lactate production. Very recent studies using a home built solenoidal coil for the NMR probe (optimized for the human lens) mounted transaxially to the magnetic field have permitted P-31 NMR measurements on a single lens. (We wish to thank Dr. J. Eliason of the Stanford Eye Bank for help in obtaining human lenses, and Santa Cruz area ophthalmologists for providing cataractous lenses. This work was supported by the American Diabetes Assoc. (to T.S.). L.T.C. was supported by NIH grants EY-01276 and EY-03247.)

W-AM-Po158 MODIFICATION OF LACTATE DEHYDROGENASE IN BOTH CHEMICALLY AND VIRALLY TRANSFORMED CELL LINES. Ann E. Kaplan, Philip Hanna, Bruce Hochstadt and Harold Amos, National Cancer Institute, NIH, Bethesda, MD 20205 and Department of Microbiology, Harvard Medical School, Boston, MA 02115.

Kinetic and molecular results identify differences in lactate dehydrogenase (LDH, E.C. 1.1.1.27) from TRL 12-13, a control cell line established from ten day old rat hepatocytes, and NMU-3, a cell line transformed in vitro by exposing TRL cells to nitrosomethylurea. With transformation, LDH activity increases per cell. Kinetically, the enzyme shows a loss of inhibition with NAD^+. The molecular forms of LDH from NMU-3 show qualitative relationships with TRL 12-13 by gel electrophoresis and isoelectric focussing methods, but only one molecular form of the enzyme increases. Using methods developed for the chemically transformed cell lines, we compared molecular forms of LDH in NIL cells and in the polyoma-transformed line, NIL-PY. Here again, both enzyme extracts show a molecular relationship to each other (but not to the hepatocyte lines) by the above methods. However, in these cell lines as well, only one molecular form appears to increase with viral transformation. The results of LDH studies with these control and transformed cell lines of different origin and transformed by different means demonstrate (1) the transformed cell lines each retain molecular identification with their nontransformed cell lines; (2) in each case, one molecular type of LDH, already present in the control cell appears to increase with transformation. From the present results we cannot ascertain whether the modification of LDH arises from genetic or metabolic influences or from both.

W-AM-Po159 PYRENEBUTYRYLCARNITINE AND COA: FLUORESCENT PROBES FOR LIPID METABOLITE MEMBRANE INTERACTION. Paul E. Wolkowicz, Depts. of Medicine, Biochemistry, Baylor Col. of Med., Hou., TX 77030.

Membrane properties of the amphipathic metabolites, fatty acyl-CoA and acylcarnitine, have been studied using pyrenebutyryl-CoA (PB-CoA) and pyrenebutyrylcarnitine (PBC). These molecules have the spectroscopic properties of pyrene, and exhibit biological and chemical characteristics related to the acylesters. PBC is more soluble in nonpolar solvents than PB-CoA, and critical micelle concentrations of both compounds resemble the medium chain fatty acylesters. PB-CoA inhibits active mitochondrial respiration noncompetitively (K_I=2μM) and mitochondrial carnitine palmitoyl- and octanoyltransferase competitively (K_I=2.1μM and 15 μM, respectively). PBC does not inhibit carnitine palmitoyltransferase or active mitochondrial respiration using glutamate-malate or succinate (+ rotenone) as respiratory substrate. PBC is a potent inhibitor of active respiration with either palmitoylcarnitine (I_{50}=1.4μM) or octanoylcarnitine (I_{50}=40 nM) as respiratory substrate. The mitochondrial carnitine acylcarnitine translocase is competitively inhibited by PBC with K_I=0.6μM for palmitoylcarnitine exchange and 23 nM for carnitine exchange. PBC and PB-CoA exhibit excimer and monomer fluorescence, the relative intensities of which are functions of their microenvironment and microscopic concentrations. PB-CoA is accessible only to the outer half of artificial lipid vesicles while PBC may cross lipid vesicle bilayers. PBC in the inner half of the bilayer appears "trapped", i.e. is inaccessible to removal by exogenous bovine serum albumin which binds PBC. These derivatives will allow study of membrane interactions of fatty acylesters central to lipid metabolism. (Supported by the American Heart Association, Texas Affiliate, NIH Grant HL 23161, and the Muscle Dystrophy Association.)

W-AM-Po160 THE ROLE OF MAGNESIUM ION ON THE HYDROLYSIS OF ATP. Setareh A. Marvasti. Department of Chemistry, Rutgers University, Piscataway, N.J. 08854.

An innovative analytical method, whereby both binding constants and rate constants could be calculated, was developed through the use of kinetic measurements for ATP hydrolysis by magnesium ion. As such, it was possible to do a quantitative interpretation of the kinetic results by calculating the rate contribution of each complex species.

Various concentrations of the tetramethylammonium salt of ATP solutions containing different concentrations of total magnesium ion were degraded in a 0.2M tetramethylammonium chloride solution with a 0.05M concentration of tris buffer. ATP and ADP that were present in the degraded solutions were separated by ion-exchange chromatography followed by ultraviolet monitoring of the column effluent.

As a result of this research, the role of magnesium ion on the hydrolysis of ATP was found to be very significant. During this study, a method was developed for the handling and the storage of unstable nucleotides for extended periods of time. (Supported by NIH GM 12307 granted to Professor Ulrich P. Strauss).

W-AM-Po161 INHIBITION OF ELECTRON TRANSFER REACTIONS IN *Paracoccus denitrificans* by 5-n-ALKYL-6-HYDROXY-4,7-DIOXOBENZOTHIAZOLES. D. Godde, C.A. Edwards, E.A. Berry, and B.L. Trumpower, Department of Biochemistry, Dartmouth Medical School, Hanover, NH 03755

A homologous series of 5-n-alkyl-6-hydroxy-4,7-dioxobenzothiazoles (X-HDBT, were X = 7, 9, etc) inhibit respiratory chain electron transfer reactions in membranes from *P. denitrificans* grown aerobically on succinate. The most potent homologues, containing 11, 13, or 15 carbon sidechains, inhibit succinate oxidase, succinate-cytochrome c reductase, and ubiquinol-cytochrome c reductase activities. Under comparable conditions of pH and enzyme concentration the X-HDBT's do not inhibit succinate-ubiquinone reductase activity. Addition of 15-HDBT to *P. denitrificans* respiring on succinate causes a decrease of the steady state level of reduction of the c cytochromes and no significant change in the redox poise of cytochrome b. The efficacy of inhibition of cytochrome c reductase activities is affected by the length of the alkyl sidechain and by the pH of the reaction mixture (see Abstract by Edwards et al.). These effects of X-HDBT on *P. denitrificans* are generally identical to those observed in mammalian mitochondria and thus further illustrate the similarities of these respiratory chains. In light of evidence that X-HDBT's inhibit cytochrome c reductase activities of mitochondrial cytochrome c reductase complex by binding to the iron-sulfur protein of the b-c_1 complex (Bowyer, J.R., Edwards, C.A., Ohnishi, T. and Trumpower, B.L., submitted), these results imply that the respiratory chain of *P. denitrificans* contains a functionally similar iron-sulfur protein. (Supported by NIH Grant GM-20379)

W-AM-Po162 A PROTON MOTIVE FORCE TRANSDUCER AND ITS POSSIBLE ROLE IN PROTON PUMPS, PROTON ENGINES, TOBACCO MOSAIC VIRUS ASSEMBLY, AND HEMOGLOBIN ALLOSTERISM. A. Keith Dunker, Washington State University, Pullman, WA 99164.

Given the usual role of prolines as helix breakers, it is surprising to find about 2 prolines deeply embedded in the membrane-spanning, probably α-helical portion of the bacteriorhodopsin molecule. This finding and several other observations lead to the question, how might prolines in α-helices be involved in proton-mediated energy transduction?

Due to the absence of a proton on the proline nitrogen, a proline-containing α-helix has a "proton hole" between the proline nitrogen and the carbonyl oxygen four residues earlier in the sequence. Here I propose a model in which the paramount feature is the change in pKa associated with a change in geometry of the proton hole.

Order of magnitude calculations suggest that the proton hole should change its pKa by about 8 units for every 10 kcal of distortion energy. Furthermore, calculations also show that it should be energetically feasible to modulate the pKa of this site over the pKa = 2-14 range. This site therefore has ideal properties to serve as the basis of an integral proton injector, an abstract model for proton pumps and engines suggested on purely theoretical grounds by Nagle and Mille (J. Chem. Phys. 74, 1367-1372, 1981).

X-ray crystallography of hemoglobin and of tobacco mosaic virus reveals structural changes that I interpret in terms of protonation and deprotonation of proton holes in proline-containing α-helices. If true, protonation and deprotonation of these proton holes account for important proton-mediated conformational changes necessary for hemoglobin allosterism and for tobacco mosaic virus assembly.

W-AM-Po163 H^+/O STOICHIOMETRY IN BEEF HEART SUBMITOCHONDRIAL PARTICLES. H. James Harmon, Depts. of Physics and Zoology, Oklahoma State University, Stillwater, OK 74078

Coupled submitochondrial particles (SMP) that are essentially completely inverted can be isolated from beef heart mitochondria following sonication. Respiratory control indices (uncoupler stimulated/oligomycin-inhibited respiratory rates) up to 6 have been measured. Addition of ADP + Pi to respiring SMP results in 1.8-fold stimulation of NADH oxidase activity. Following two washes with 0.15 M KCl-containing medium, addition of exogenous cytochrome c results in less than 6% stimulation of respiratory activity. This indicates that the vesicles are greater than 94% inverted. H^+/O ratios were determined by the oxygen pulse method in 0.15 M KCl medium in the presence of valinomycin using succinate as substrate to achieve anaerobiosis. H^+/O ratios for succinate oxidase in SMP are at least 8 and have been observed as high as 10. Protons are not translocated in the presence of CCCP. Neither the addition of oligomycin nor the addition of ADP + Pi alters the proton stoichiometry. This provides independent evidence that in beef heart submitochondrial membranes the H^+/O ratio for sites II and III averages at least 4. Further, this stoichiometry is obtained in the absence of transport inhibitors. N-ethylmaleimide has no effect on H^+/O ratios.

This work was supported by a Grant-in-Aid from the American Heart Association and with funds contributed in part by the Oklahoma Affiliate.

W-AM-Po164 IDENTIFICATION OF CYSTEINE AND HISTIDINE LIGANDS OF Cu_a BY ELECTRON NUCLEAR DOUBLE RESONANCE (ENDOR) OF ISOTOPICALLY ENRICHED YEAST CYTOCHROME c OXIDASE. T. H. Stevens, C. T. Martin, H. Wang, and S. I. Chan, Dept. of Chem., Caltech, Pasadena, CA 91125; C. P. Scholes, Dept. of Physics, SUNYA, Albany, NY 12222.

ENDOR of protons and nitrogens was obtained from the EPR-detectable Cu_a center in yeast cytochrome c oxidase. With ^1H and ^{14}N in their natural ~100% abundance, these signals are similar to those previously reported from beef heart oxidase (Van Camp et al, BBA, 537 (1978) 238). Strongly coupled proton resonances occur in the 19-22 MHz region, weakly coupled protons near the free proton frequency (~14 MHz), and ^{14}N ENDOR occurs in the 7-10 MHz region.

To identify proton and nitrogen-containing ligands, two separate isotopically-enriched samples were grown and isolated. First, cysteine auxotrophs were grown on cysteine which was 90% deuterated on the β-carbon adjacent to the thiol sulfur; i.e., grown on CD_2-cys instead of CH_2-cys. Second, histidine auxotrophs were grown on histidine that was 95% $^{15}N_2$ on both imidazole ring positions. In the CD_2-cys oxidase, the ENDOR signal from the strongly coupled protons in the 19-22 MHz region was substantially diminished. In the ^{15}N-his oxidase, the characteristic ^{14}N ENDOR in the 7-10 MHz region disappeared and was replaced by ENDOR intensity in the 11-13 MHz region, as expected for the ^{15}N nucleus which has a 40% larger nuclear magnetic moment than ^{14}N. Thus Cu_a has at least one cysteine and one histidine ligand. Furthermore, the strong hyperfine coupling to the cysteine β-carbon proton(s) indicates substantial spin delocalization onto a cysteine sulfur ligand of the oxidized Cu_a site. (Work supported by NIH grants AM-17884 and GM-22342.)